

OPTICAL PUMPING

I. INTRODUCTION

The term “optical pumping” refers to a process which uses photons to redistribute the states occupied by a collection of atoms. For example, an isolated collection of atoms in the form of a gas will occupy their available energy states, at a given temperature, in a way predicted by standard statistical mechanics. This is referred to as the thermal equilibrium distribution. But the distribution of the atoms among these energy states can be radically altered by the clever application of what is called “resonance radiation”.

Alfred Kastler, a French physicist, introduced modern optical pumping in 1950 and, in 1966, was awarded a Nobel Prize “*for the discovery and development of optical methods for studying Hertzian resonances in atoms.*” In these laboratory experiments, you will explore the phenomenon of optical pumping and its application to fundamental measurements in atomic physics using an apparatus built by TeachSpin¹. It is not likely that you will have time to study all the possible experiments that this instrument is capable of performing, but you should have ample opportunity to explore many interesting phenomena. The apparatus has deceptively simple components, yet it is capable of exploring very complex physics.

The atom you will be exploring is rubidium. It is chosen because of its hydrogen-like qualities. That is, it is a very good approximation to consider this atom as a one-electron atom, since the core electrons form a closed shell, noble gas configuration. The rubidium atoms are contained within a sealed glass bulb along with the noble gas neon at about 0.04 atm pressure. Ideally, if one were studying the metrology of the energy state of rubidium, one would want to have the atoms in vacuum at extremely low density, so they would not interact. Such systems do exist; they are called an atomic beam apparatus, but they are very large and expensive instruments which have their own serious limitations. The addition of neon as a buffer gas, in a small contained volume, greatly simplifies the apparatus and the experiments. Because of the spherical symmetry of the electronic ground state of neon, collisions between a rubidium and neon atom do not exchange angular momentum. This turns out to be crucial for performing optical pumping experiments.

Optical pumping is the basis of all lasers; it is an important tool for studying collision and exchange relaxation processes, and also finds applicability in both solid state and liquid state physics. Although the basic process was discovered over 50 years ago, the topic is very current.

¹<http://www.teachspin.com>. This revised lab manual is based on TeachSpin's “Guide to the Optical Pumping Experiment”.

(i) Structure of alkali atoms

In these experiments, we will study the absorption of light by rubidium atoms, and as a prelude to that, we will consider the atomic structure of the rubidium atom. In the quantum mechanical model we will consider, atoms are described in terms of the central field approximation in which the nucleus is taken to be a point particle characterized by its only observable properties of charge, spin angular momentum, and electric and magnetic moments. The energy levels can be described by angular momentum wave functions that can be calculated generally from the angular parts of the separated Schrodinger equation. These functions are applied in a perturbation theory approach to calculate the eigenstates of the atom. In the case of the alkali atoms, the angular momenta are coupled in what is called the Russell-Saunders coupling scheme, which yields energy level values close to the observed.

All of the alkali atoms are similar in structure to the hydrogen atom. That is, many of their properties are determined by a *single* valence electron. Rubidium, which has an atomic number of 37, can be described by means of an electronic configuration (in the standard notation):

$$1s^2 2s^2 2p^6 3s^2 3p^6 3d^{10} 4s^2 4p^6 5s$$

where the superscripts are the number of electrons in each shell. The electrons in the inner shells are paired, and to the approximation necessary here, we can completely neglect the presence of the inner electrons, and concentrate our attention on the single outer electron. That is, the entire discussion of all our optical pumping experiments will be based on a model that considers a free rubidium atom as if it was a simple hydrogenic single electron atom.

The outer electron can be described by means of an orbital angular momentum \mathbf{L} , a spin angular momentum \mathbf{S} , and a total non-nuclear angular momentum \mathbf{J} , all in units of \hbar . Since these are all vectors they can be combined by the usual rules as shown in Figure 1. Each of these angular momenta has a magnetic dipole moment associated with it, and they are coupled by a magnetic interaction of the form $\boldsymbol{\mu}_L \cdot \boldsymbol{\mu}_S$. This interaction is due to the electron's spin and the magnetic field it sees as the charged proton moves around it. As is the case with classical angular momenta, different orientations of the vectors lead to different interaction energies. Here, however, the values of energy that result are quantized, and can have only allowed values. As can be seen from Figure 1, the total angular momentum can be written as:



Fig. 1. Angular momentum coupling in the valence electron of an alkali atom.

$$\mathbf{J} = \mathbf{L} + \mathbf{S} \quad (1)$$

In the absence of any further interactions, \mathbf{J} will be a constant of the motion. In the electronic ground state of an alkali atom, the value of \mathbf{L} is zero as it is in the hydrogen atom. Since a single electron has an intrinsic spin angular momentum of $\hbar/2$, the value of \mathbf{S} will be $1/2$, and the total angular momentum will have a value of $S = 1/2$.

In spectroscopic notation, the electronic state is written $^{2S+1}L_J$ so that the ground state of an alkali atom is designated $^2S_{1/2}$. The first excited state has an L value of $1 \hbar$, and is designated as a P state. Higher values of L are given the label D, F, \dots by convention.

In the case of the P state, J can only have the values $L + S$ and $L - S$. Thus, there are the two states, $^2P_{1/2}$ and $^2P_{3/2}$, for the single electron in an alkali atom. These states have different energies. This energy splitting is called the “Fine structure”, and is shown diagrammatically in Figure 2. Please note, Figure 2 is not to scale! The fine structure splitting is much, much, much, smaller than the energy difference between the ground state and the first excited state.

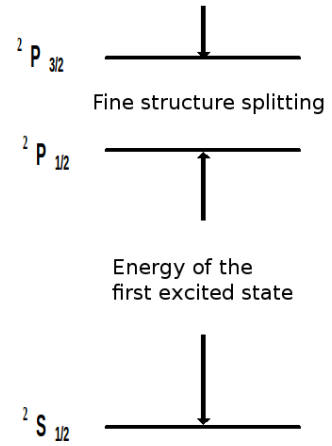
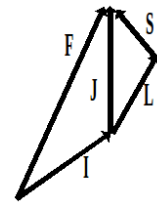


Fig. 2. Energy level diagram of an alkali atom.

Associated with this spin is a magnetic dipole moment. In the approximation that we are considering here, the nuclear moment will couple with the electronic magnetic dipole moment associated with J to form a total angular momentum of the atom, F . In the context of the vector model, the coupling is as shown in Figure 3.



The nuclear spin is denoted by I , the interaction is again of the form $\mu_I \mu_J$, and the result is a further splitting of the energy levels called the “Hyperfine structure”. This energy can be characterized by a Hamiltonian as:

Fig. 3. Hyperfine coupling in an alkali atom.

$$H = ha \mathbf{I} \cdot \mathbf{J} \quad (2)$$

where h is Planck’s constant and a is a constant that is different for each electronic state and is determined experimentally. The eigenvalues of this Hamiltonian give the interaction energies as shown in Figure 4.

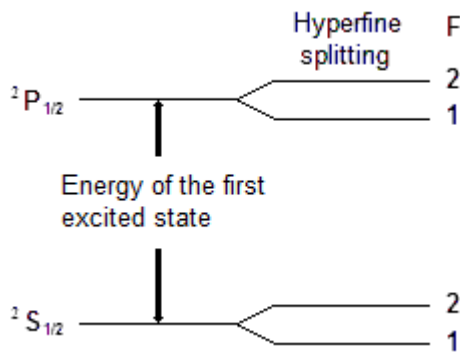


Fig. 4. Hyperfine splitting for $I = 3/2$.

(ii) Interaction of an alkali atom with a magnetic field

We must now consider the effect of a weak external magnetic field on the energy levels of our alkali atom. This will produce the Zeeman effect, and will result in further splitting of the energy levels. What is meant by “weak” magnetic field? If the resulting splitting is very small compared to the Hyperfine splitting, the magnetic field is said to be weak. This will be the case in all the experiments discussed here.

A vector diagram for an alkali atom is shown in Figure 5. \mathbf{B} designates the magnetic field, and M is the component of \mathbf{F} in the direction of the magnetic field. \mathbf{F} precesses about the magnetic field at the Larmour frequency.

The Hamiltonian that accounts for the interaction of the electronic and nuclear magnetic moments with the external field is:

$$H = ha \mathbf{I} \cdot \mathbf{J} - \frac{\mu_J}{J} \mathbf{J} \cdot \mathbf{B} - \frac{\mu_I}{I} \mathbf{I} \cdot \mathbf{B} \quad (3)$$

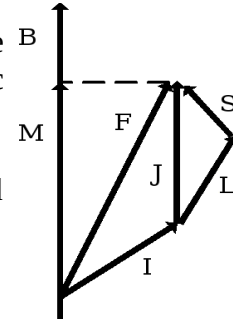


Fig. 5. Zeeman effect in an alkali atom.

where μ_J is the total electronic magnetic dipole moment (spin coupled to orbit), and μ_I is the nuclear magnetic dipole moment. The resulting energy levels are shown in Figure 6 for the $^2S_{1/2}$ ground electronic state with a positive nuclear magnetic moment and a nuclear spin of $3/2$. The levels are similar for the $^2P_{1/2}$ state. For reasons that will become clear later, we will ignore the $^2P_{3/2}$ state. As can be seen from Figure 6, the magnetic field splits each F level into $2F + 1$ sublevels that are approximately equally spaced. In actuality, they vary in their spacing by a small amount determined by the direct interaction of the nuclear magnetic moment with the applied field. We will take advantage of this later on to allow all of the possible transitions to be observed.

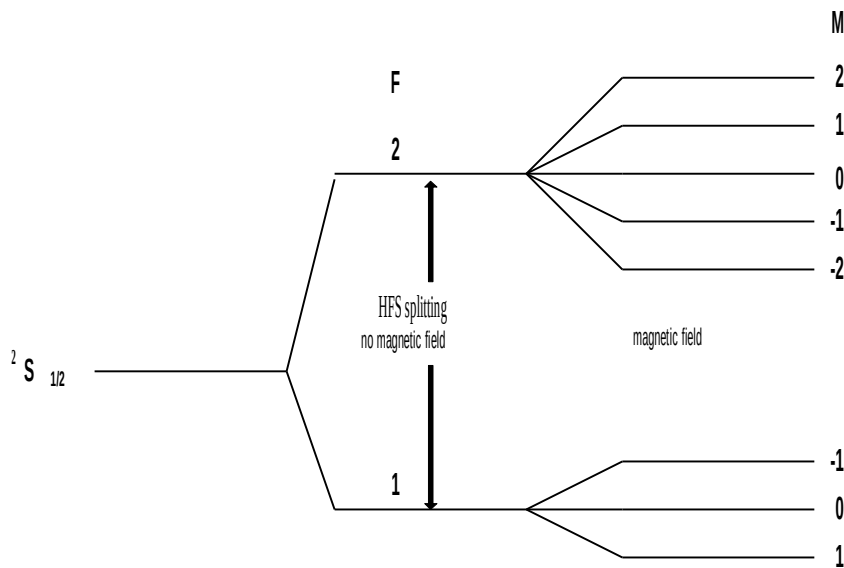


Fig. 6. Energy levels of an alkali atom in the $2S_{1/2}$ state with a nuclear spin of $3/2$ and a positive nuclear magnetic dipole moment in a weak magnetic field.

In the case of an atom with either $J = 1/2$ or $I = 1/2$, the energy levels can be calculated in closed form from quantum mechanics. This solution is called the Breit-Rabi equation. To proceed further, we need to consider the atom-magnetic field interaction in more detail. A single electron has spin of $1/2$ and an electrical charge of about 1.6×10^{-19} Coulombs. In the simplest picture, this rotating charge gives rise to a magnetic dipole moment whose magnitude is equal to μ_B , the Bohr magneton. If the electron is bound in an atom, its effective magnetic moment changes and is best described by means of the Lande g -factor.

If the nucleus is neglected, the vector model is used to write the energy of interaction of an atom with an external magnetic field as:

$$\text{Magnetic Energy} = \frac{M(\mathbf{L} + 2\mathbf{S}) \cdot \mathbf{J}}{J^2} \mu_B B = g_J \mu_B MB \quad (4)$$

where g_J , known as the Lande g -factor, is given by:

$$g_J = \frac{(\mathbf{L} + 2\mathbf{S}) \cdot \mathbf{J}}{J^2} \quad (5)$$

This can be evaluated from the vector model to be:

$$g_J = 1 + \frac{J(J+1) + S(S+1) - L(L+1)}{2J(J+1)} \quad (6)$$

In terms of this g -factor, the interaction energy of the electronic spin with a magnetic field can be expressed as:

$$W = -g_J \mu_B MB \quad (7)$$

where B is the magnitude of the magnetic field and M is the component of the electron spin along the magnetic field. In the case of rubidium, where $J = S = 1/2$, the Lande g -factor is 2. Actually, the measured g -factor turns out to be 2.00232.

If the interaction with the nucleus is considered, the g -factor is given by:

$$g_F = g_J \frac{F(F+1) + J(J+1) - I(I+1)}{2F(F+1)} \quad (8)$$

The interaction energy is then given by:

$$W = -g_F \mu_B MB \quad (9)$$

where the direct interaction of the nuclear moment with the magnetic field is being neglected.

The above results are satisfactory as long as the interaction energy with the magnetic field is small, and the energy levels depend only linearly on the magnetic field. For the purposes of our experiment, we need to consider terms quadratic in the field. Equation 3 can be diagonalized by standard methods of perturbation theory. The result is the Breit-Rabi equation:

$$W(F, M) = -\frac{\Delta W}{2(2I+1)} - \frac{\mu_I}{I} MB \pm \frac{\Delta W}{2} \left[1 + \frac{4M}{2I+1} x + x^2 \right]^{1/2} \quad (10)$$

where

$$x = (g_J - g_I) \frac{\mu_B B}{\Delta W}, \quad g_I = -\frac{\mu_I}{I\mu_B} \quad (11)$$

W is the interaction energy and ΔW is the hyperfine energy splitting.

A plot of the Breit-Rabi equation is shown in Figure 7. The energy is shown on the vertical axis field as the dimensionless number $W/\Delta W$, and the horizontal axis shows the magnetic field. The diagram can be divided into three main parts. The first is the Zeeman region very close to $x = 0$ where the energy level splitting varies linearly with the applied magnetic field. The second is the Paschen-Back region $x > 2$, where the energy levels are again linear in the magnetic field. This corresponds to the decoupling of I and J . The upper group of four levels corresponds to m_J , the projection of J along the axis of the applied magnetic field, having a value of $1/2$, while the four lower levels correspond to $m_J = -1/2$. The individual levels correspond to different values of m_I , the projection of I along the axis of the applied magnetic field.

The third region is the intermediate field region that extends from the Zeeman to the Paschen-Back region. Here the energy levels are not linear in the applied magnetic field; I and J are decoupling, and M is no longer a “good” quantum number. In the Zeeman region, M is a good quantum number. At high fields m_I and m_J are good quantum numbers and can be used to label the levels. At all fields $M = m_I + m_J$.

In the optical pumping experiment, we will be concerned with small magnetic fields, where the levels are either linear in the magnetic field, or where there is a small quadratic dependence.

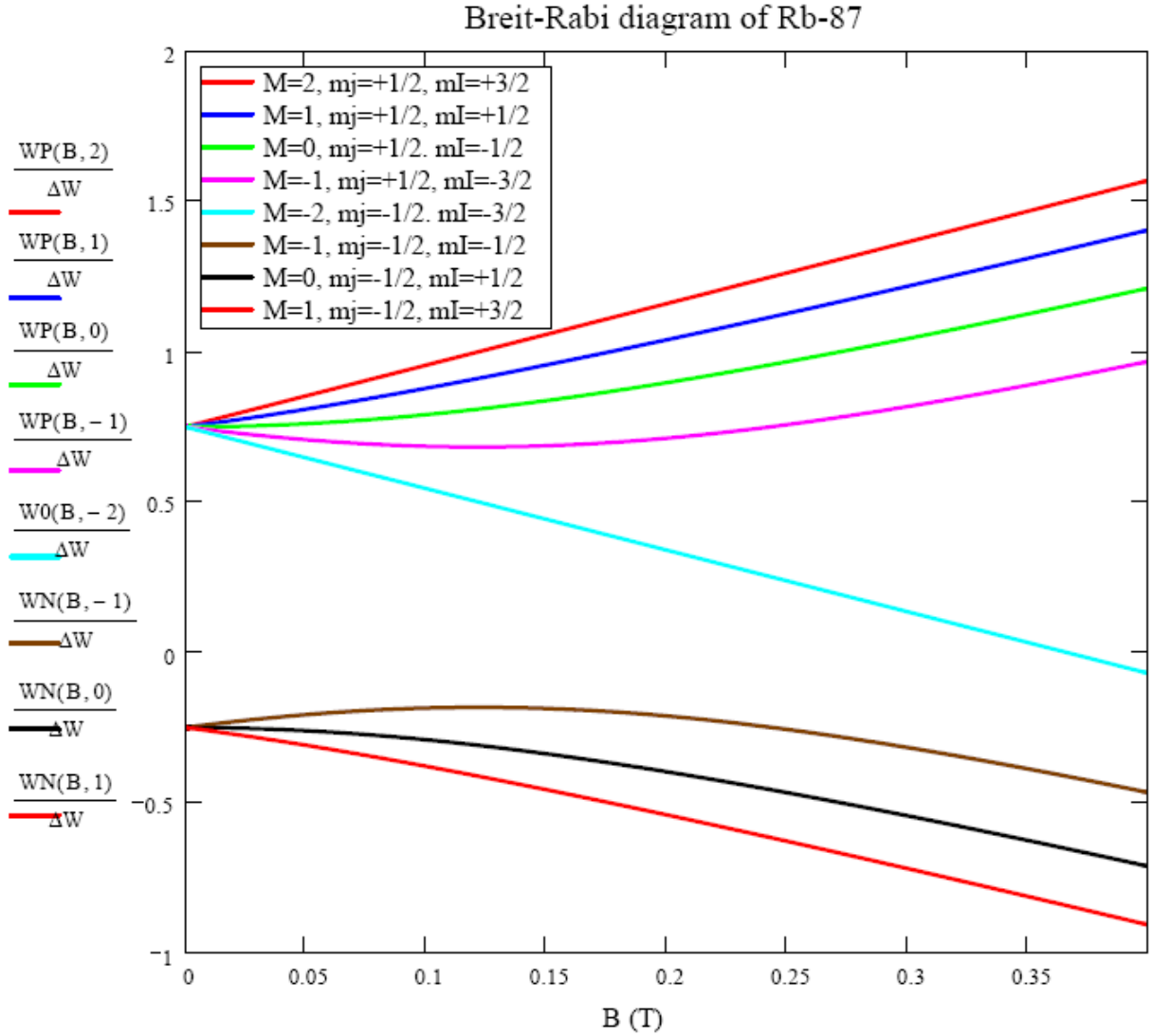


Fig. 7. Breit-Rabi diagram of Rb⁸⁷ in a magnetic field.

(iii) Photon absorption in an alkali atom

The three lowest electronic states of an alkali atom are shown in Figure 8. As discussed there, if all filled electron shells are omitted, these three states can be labeled as:

ground electronic state: $5s \ ^2S_{1/2}$
 first excited electronic state: $5p \ ^2P_{1/2}$
 second excited electronic state: $5p \ ^2P_{3/2}$

An electric dipole transition can take place between S and the P states with the selection rules $\Delta L = 0, \pm 1$ but not $L = 0$ to $L = 0$, $\Delta S = 0$, and $\Delta J = 0, \pm 1$. Thus, this type of transition can occur from the ground state to both of the excited states.

In the optical pumping experiment we are primarily interested in the absorption of light by a volume of a gas as illustrated in Figure 8.

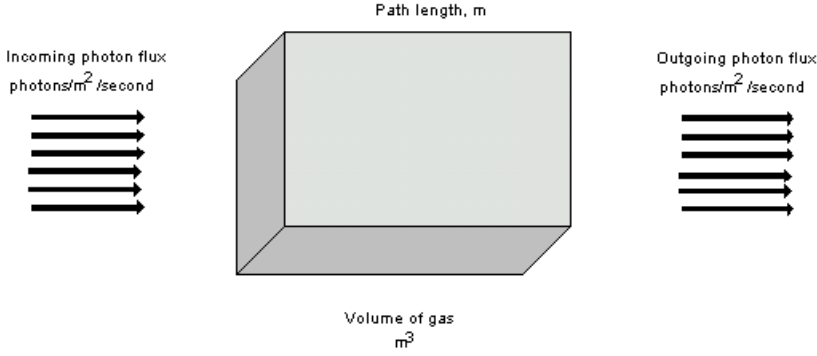


Fig. 8. Light absorption by a volume of gas.

Assuming that the light is resonant with one of the above transitions, a fraction of the incident light will be absorbed by the atoms of the gas. Once the atoms have been excited they will decay back to the ground state by spontaneous emission, but since this emission occurs equally in all directions, only a small amount will be radiated into the outgoing beam. For our discussion, this fraction will be ignored.

It is convenient to describe this process using the concept of a “cross section”. Suppose, for instance, that the incoming beam consisted of electrons instead of photons. In that case, the attenuation of the incoming electrons by the gas atoms can, in the limit of low density, be described by the simple relation:

$$n = n_0 e^{-\sigma \rho l} \quad (12)$$

where n_0 and n are the incident and outgoing flux of electrons, ρ is the gas density, l is the path length through the gas, and σ is the cross section. In the case of electron-atom or atom-atom scattering, the magnitude of the cross section is of the order of 10^{-20} m^2 , which is roughly the cross sectional area of an atom with geometrical diameter 10^{-10} m .

A similar concept can be applied to the absorption of photons by a volume of gas. Here we write:

$$I = I_0 e^{-\sigma_0 \rho l} \quad (13)$$

where I_0 and I represent the incident and outgoing flux of photons. If the incident photons are resonant with an atomic transition, the observed cross-section will be dramatically different from the geometrical cross-section. In fact, this cross-section is often taken to be of the order of the wavelength of the radiation squared. In this experiment, you will attempt to measure the photon absorption cross-section for rubidium resonance radiation on rubidium atoms, and you can compare your measured value with expectations.

The quantity σ_0 is the maximum absorption cross-section measured at the center of the atomic resonance, and it is related to the usual definition of the absorption coefficient by:

$$k_0 = \sigma_0 \rho \quad (14)$$

For an absorption line that is being broadened only by the Doppler effect, the maximum absorption coefficient can be calculated from:

$$k_0 = \frac{2}{\Delta\nu_D} \frac{\lambda_0^2 g_2}{8\pi g_1} \frac{\rho}{\tau} \quad (15)$$

where λ_0 is the wavelength at the center of the absorption line, $\Delta\nu_D$ is the Doppler width of the absorption line, g_1 and g_2 are the statistical weights of the lower and upper state respectively, and τ is the radiative lifetime of the upper electronic state. The Doppler width can be calculated from:

$$\Delta\nu_D = 3 \times 10^{-20} \nu_0 \left(\frac{T}{M} \right)^{1/2} \quad (16)$$

where ν_0 is the transition frequency, T is the absolute temperature of the absorbing gas, and M is the mass of the absorbing atom.

For optical pumping, we must take the hyperfine structure into account. Now an additional selection rule, $\Delta F = 0, \pm 1$, must be added for changes in the total angular momentum quantum number. Additional splitting is introduced by an external magnetic field, requiring yet another selection rule $\Delta M = 0, \pm 1$. Thus, the selection rules for an electric dipole transition can be summarized by:

Electric dipole transition: $\Delta S = 0, \Delta J = 0, \pm 1, \Delta L = 0, \pm 1$ but not $L = 0$ to $L = 0$
 $\Delta F = 0, \pm 1$ and $\Delta M = 0, \pm 1$

In the emission spectrum of an alkali atom, all transitions obeying the above selection rules are observed, and these give rise to the well-known bright line spectrum (the emission Zeeman effect will be ignored in this discussion). In absorption, however, things can be somewhat different in regard to the selection rule for M . Since angular momentum must always be conserved, the absorption of light in the presence of an applied magnetic field will depend on the polarization of the light and the direction of the incoming beam of light with respect to the direction of the magnetic field. For our purposes, we are only interested in the absorption of circularly polarized light that is resonant with the transition from the $^2S_{1/2}$ state to the P states.

In the optical pumping experiment, the direction of the incident light is parallel to the applied magnetic field, and the light is polarized so that it is either right or left circularly polarized. In this arrangement only transitions in which M changes by $+1$ or -1 are allowed, but not both. Pumping will occur in either case as will be discussed later.

The above discussion applies to allowed electric dipole transitions in an atom. We must also consider magnetic dipole transitions that are about 10^5 times weaker than in the electric dipole case. The transitions in which we will be interested occur in the hyperfine structure and between the magnetic sublevels, and will only be observed in absorption. The selection rules are $\Delta F = 0, \pm 1$ and $\Delta M = 0, \pm 1$. Which transitions occur depends on the orientation of the RF magnetic field with respect to the DC magnetic field.

In our experiment, the RF magnetic field is perpendicular to the DC magnetic field. In this case, the only transitions that can occur have $\Delta F = 0, \pm 1$ and $\Delta M = \pm 1$. The $\Delta F = \pm 1$ transitions occur at RF frequencies of several gigahertz (GHz), and can not be observed with this apparatus. Therefore we will only be concerned with $\Delta F = 0$ and $\Delta M = \pm 1$.

In the case of allowed electric dipole transitions in emission, the lifetimes of the excited states are of the order of 10^{-8} second, resulting in a natural line width of several hundred megahertz (MHz). The actual line width, determined by Doppler broadening, is of the order of one GHz. For magnetic dipole transitions in the hyperfine structure of the ground electronic state, the lifetimes for radiation are much longer, and collision processes will determine the actual lifetimes.

(iv) Optical pumping in rubidium

Optical pumping is a method of driving an ensemble of atoms away from thermodynamic equilibrium by means of the resonant absorption of light. Rubidium resonance radiation is passed through a heated absorption cell containing rubidium metal and a buffer gas. The buffer gas is usually a noble gas such as helium or neon. If it were not present, the rubidium atoms would quickly collide with the walls of the cell which would tend to destroy the optical pumping. Collisions with the buffer gas are much less likely to destroy the pumping, thus allowing a greater degree of pumping to be obtained. The general arrangement of the apparatus is shown in Figure 9.

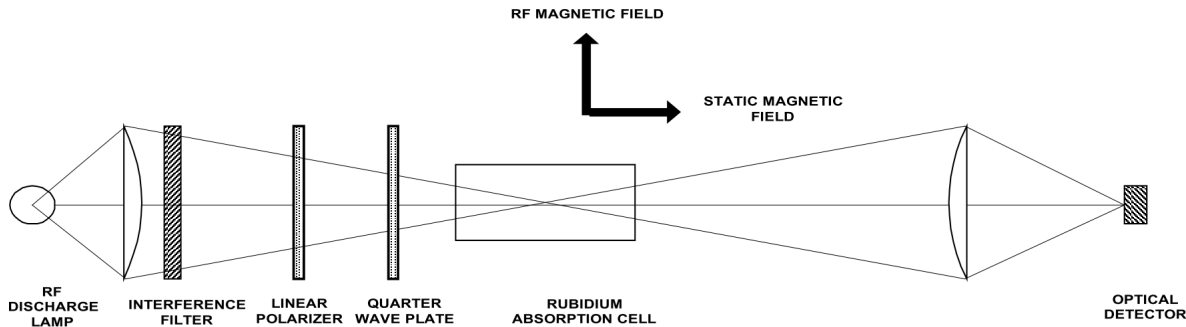


Fig. 9. Apparatus arrangement for optical pumping.

Resonance light is produced by an RF discharge lamp containing xenon gas and a small amount of rubidium metal, which has been enriched in Rb^{87} , such that there are equal amounts of natural Rb and Rb^{87} . The gas is excited by an oscillator operating at a frequency of about 100 MHz. The high electric field produced in the lamp causes ionization in the gas, and the resulting electrons are accelerated sufficiently to excite the rubidium atoms by collisions. Spontaneous radiation from the excited states produces the emission spectrum of rubidium.

Resonance light from the lamp consists of two main lines, one at 780 nm and one at 795 nm. The 780 nm line is removed by the interference filter and the remaining light is circularly polarized before being passed through the absorption cell. An optical detector monitors the intensity of the transmitted light. A DC magnetic field is applied to the absorption cell along the optical axis, and transitions are induced in the sample by means of a transverse RF magnetic field.

Figure 10 shows the magnetic fields and angular momenta involved in the optical pumping of rubidium. The projection of F along the magnetic field is the magnetic quantum number M , and this vector precesses about the applied magnetic field at the Larmour frequency. Note that the RF magnetic field is perpendicular to the applied DC magnetic field. **Transitions are induced between electronic energy levels by the optical radiation and between the Zeeman levels by means of the RF magnetic field.** The optical transitions are shown schematically in Figure 11 for those energy levels involved in the optical pumping of Rb^{87} , which has a nuclear spin of $3/2$. The transitions are shown for the case of $\Delta M = +1$, but the situation would be similar for $\Delta M = -1$, except that the pumping would go to the $M = -2$ level of $^2S_{1/2}$ electronic ground state.

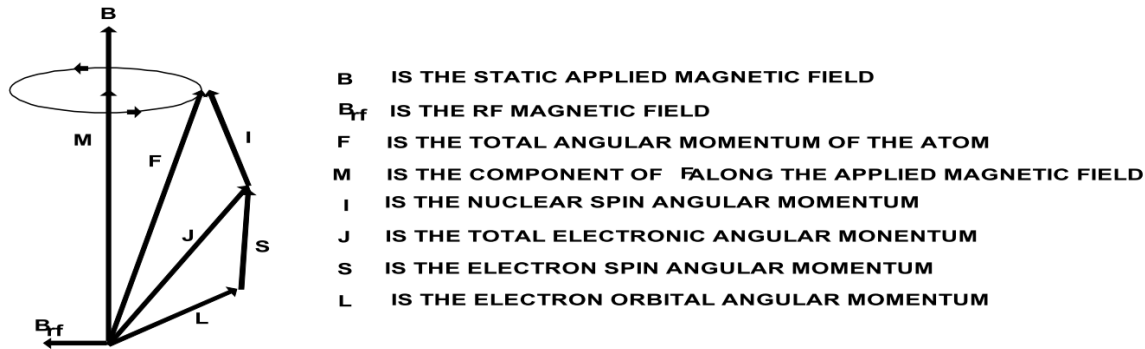


Fig. 10. Magnetic fields and angular momenta involved in the experiment.

Due to the circular polarization of the incident light, there are no transitions from the $M = +2$ magnetic sublevel of the ground state since there is no $M = 3$ state. The excited states can decay back into this level by spontaneous emission of collisions providing a path into the level but not out of it. Hence the population of this level will increase with respect to the other sublevels. The population of the $M = +2$ level is monitored by the intensity of the transmitted light, and any process that changes this population, such as transitions between the M levels, will change the intensity of this transmitted light.

The intensity of the transmitted light is monitored by a photo diode whose output is amplified and observed on an oscilloscope or other recording device. The RF is set to a predetermined frequency and amplitude, and the magnetic field is slowly varied. The resulting output represents the transmitted light intensity as a function of applied magnetic field.

ENERGY LEVELS FOR Rb^{87} ($I = 3/2$) IN AN APPLIED MAGNETIC FIELD

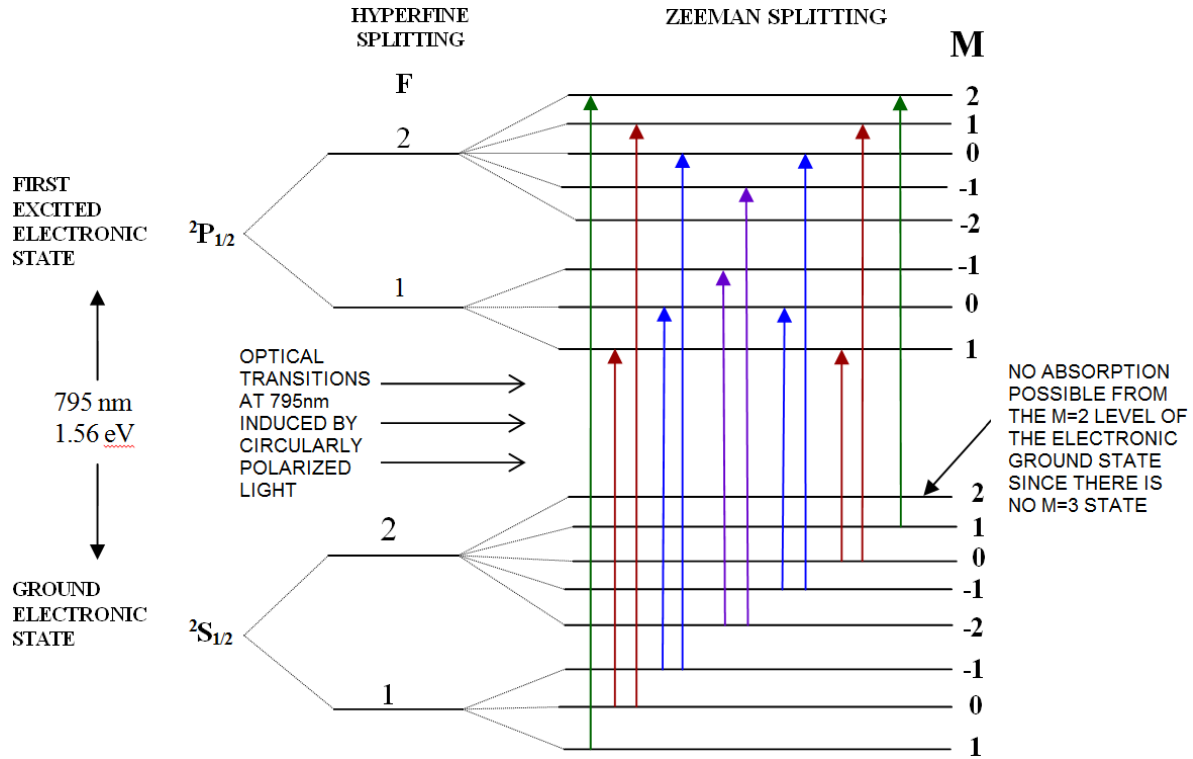


Fig. 11. Transitions involved in the optical pumping of Rb^{87} . In the absence of collisions, spontaneous emission will eventually drive the atomic population into the $M=2$ magnetic sublevel of the ground electronic state.

The optical pumping process itself will be studied in this experiment, and pumping requires a time of 10 - 20 milliseconds to achieve a suitable population of the $M = +2$ sublevel. Hence the rate of variation of the magnetic field must be kept small in order for there to be sufficient absorption of the transmitted light.

If the above discussed processes were the only ones that occurred, the result would be a very large increase in the population of the $M = +2$ or $M = -2$ states. However, we must consider collisional processes between the pumped rubidium atoms and other rubidium atoms, and also collisions with atoms of the buffer gas. These collisions can result in transitions between the magnetic substates, and such transitions will tend to equalize the populations and destroy the optical pumping. In actuality, the amount of pumping will be determined by a balance between the rate of transitions into the pumped state and the rate at which atoms are removed from this state by collisional relaxation processes.

A set of rate equations can be used to describe the pumping process. Consider the isotope Rb^{87} that has a nuclear spin of $3/2$ and a total of 8 magnetic sublevels in the ground electronic state. Let b_{ij} be the probability per unit time that an atom in the sublevel i of the ground state has undergone a transition to the sublevel j of the ground state by absorption and re-emission of a photon. Similarly let w_{ij} be the probability per unit time for the corresponding transition produced by relaxation processes.

The occupation probability $p_k(t)$ of the k -th level is obtained by the solution of the following set of eight simultaneous differential equations:

$$\dot{p}_k = - \sum_{j=1}^8 (b_{kj} + w_{kj}) p_k + \sum_{j=1}^8 (b_{jk} + w_{jk}) p_j, \quad k=1,2,\dots,8 \quad (17)$$

Only seven of these equations are independent since $\sum_k p_k = 1$. The dot denotes differentiation with respect to time, and the sums should exclude terms in which $j = k$ and $i = k$. After the pumping light is turned on, the population of the $M = +2$ or the $M = -2$ state will increase exponentially with time and the population of the other M levels will decrease. Thus, an excess population in the level of maximum M will develop as compared to the population distribution in thermodynamic equilibrium. This is what is meant by the term “optical pumping”.

(v) Zero field transition

Before we consider RF resonances in rubidium, it is necessary to discuss the transitions that can be observed at zero magnetic field. Assume that the apparatus is set up as in Figure 9 and that no RF is applied. The magnetic field is now slowly swept around zero, and the intensity of the transmitted light is monitored. A decrease in intensity will be observed as the field goes through zero as shown in Figure 12.

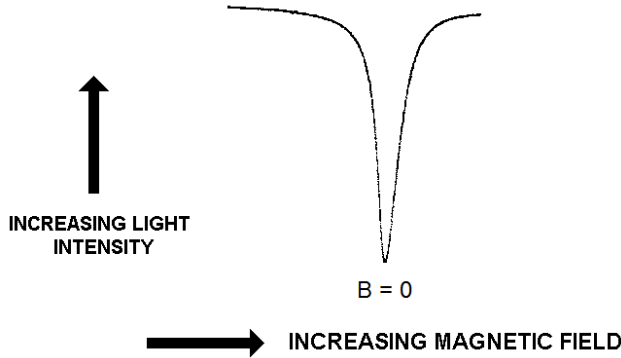


Fig. 12. Transition at zero magnetic field with no RF.

If the magnetic field is set to zero manually, a DC signal will be observed as a decrease in the intensity of the transmitted light. This can be understood qualitatively by referring to Figure 13 which shows the energy levels near zero magnetic field. To either side of zero field, the levels are split in energy, and normal optical pumping occurs. However, at or near zero field, the levels become degenerate, optical pumping does not produce a population imbalance, and more light is absorbed.

The zero field signal provides a good way to determine the parameters for zero total magnetic field within the volume of the absorption cell. If the magnetic field is swept in time and the output of the optical detector displayed on a scope, the field in the cell can be made as near zero as possible by adjusting the compensating coils and the orientation of the apparatus to achieve minimum line width. The above is true as long as the magnetic field is not swept too rapidly. Fast sweeping will produce time dependent effects which will be discussed later.

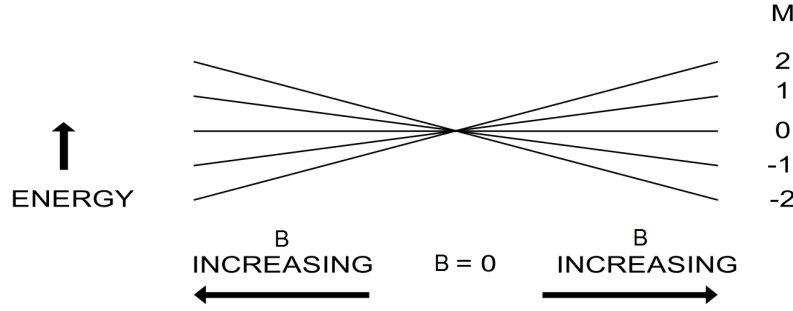


Fig. 13. Energy levels near zero magnetic field with no RF.

(vi) RF spectroscopy of Rb^{85} and Rb^{87}

As mentioned in the previous section, optical pumping drives an atomic system away from thermodynamic equilibrium. Consider the energy levels of the ground electronic state as shown in Figure 11 for Rb^{87} (nuclear spin of $3/2$). We are interested in the levels for atoms in a weak magnetic field (far right of diagram). Since $I = 3/2$ and $J = 1/2$, the total angular momentum quantum number has the values of $F = 2$ or $F = 1$. The levels would be similar for Rb^{85} except in that case $F = 3$ or 2 .

In thermodynamic equilibrium, the population of the magnetic sublevels of the ground electronic state would be essentially equal, and optical pumping will lead to an excess of population in either the $M = 2$ or the $M = -2$ levels. After the pumping light has been on for a sufficient time, of the order of milliseconds, a new equilibrium will be established, and the intensity of the light transmitted by the cell will reflect this new equilibrium. If an RF magnetic field is applied, transitions with $\Delta M = \pm 1$ will be induced, and these will tend to drive the system back toward thermodynamic equilibrium. The result will be a decrease in the intensity of the transmitted light.

Equation 9 gives the relative energy levels of the ground electronic state as $W = -g_F \mu_B MB$. We can calculate the resonance transition frequency as:

$$W(M+1) - W(M) = g_F \mu_B B(M+1) - W(M) = g_F \mu_B B \quad (18)$$

$$\nu = g_F \mu_B B / h \quad (19)$$

where ν is the transition frequency and h is Planck's constant.

The above equations are true as long as the energy levels are a linear function of the applied magnetic field. When terms quadratic in the magnetic field need to be considered, an expansion for the frequency can be used as shown in the next paragraph. At higher fields yet the full Breit-Rabi equation must be used.

To obtain an expression for the transition frequencies that is good to terms quadratic in the magnetic field, it is convenient to relabel the energy levels in terms of an average quantum number. The resonance frequencies for transitions between the levels $|F, M\rangle$ and $|F, M-1\rangle$ with energies $W(F, M)$ and $W(F, M-1)$ and mean azimuthal quantum number $\bar{M} = M - 1/2$ are:

$$\omega_{FM} = (W_{F,M} - W_{F,M-1}) / \hbar \quad (20)$$

Physically meaningful values of \bar{M} occur in the range $-I \leq M \leq I$. The resonance frequencies correct to second order in the magnetic field are given by:

$$\omega_{I+1/2, \bar{M}} = \frac{B(g_J \mu_B - 2\mu_I)}{(2I+1)\hbar} - \frac{2B^2 \bar{M}(g_J \mu_B + \mu_I/I)^2}{(2I+1)^2 \hbar^2 \omega_{hf}} \quad (21)$$

$$\omega_{I-1/2, \bar{M}} = -\frac{B(g_J \mu_B + 2\{1+1/I\}\mu_I)}{(2I+1)\hbar} + \frac{2B^2 \bar{M}(g_J \mu_B + \mu_I/I)^2}{(2I+1)^2 \hbar^2 \omega_{hf}} \quad (22)$$

where μ_B is the Bohr magneton and $\hbar\omega_{hf} = (2I+1)A/2$ is the energy splitting of the Zeeman multiplets at zero magnetic field. To first order in B , the resonance frequencies are independent of \bar{M} . To second order in B , the resonance frequencies exhibit a quadratic splitting proportional to $B^2 \bar{M}$ which is the same for both Zeeman multiplets.

(vii) Transient effects

Up until now we have been considering optical pumping only in the steady state when the RF has been on for a relatively long time. We will now consider transient phenomena.

We referred in section (iv) to the time it takes to establish equilibrium after the pumping radiation has been turned on. Here we will consider the behavior of the pumped system when the RF is rapidly turned off and on while tuned to the center of resonance. In the Zeeman region at weak magnetic fields, the resonance frequency is given by:

$$\omega_0 = 2\pi\nu_0 = g_f \frac{\mu_B}{\hbar} B_0 \quad (23)$$

Define the Gyromagnetic Ratio γ as:

$$\gamma = g_f \frac{\mu_B}{\hbar} \quad (24)$$

Then the Larmor frequency ω_0 is given by:

$$\omega_0 = \gamma B_0 \quad (25)$$

Thus γ is the atomic equivalent of the gyromagnetic ratio used in nuclear magnetic resonance.

Figure 14 shows a vector diagram of the spin and the magnetic fields that are relevant to this experiment. The vector \mathbf{B}_{RF} represents the applied RF magnetic field provided by the coils at right angles to the static field. We will assume that the magnitude of the RF magnetic field is always much smaller than that of the static field. We will also consider the problem classically.

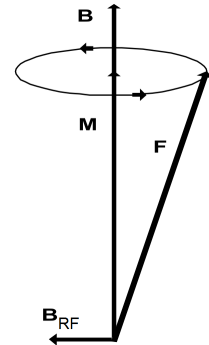


Fig. 14. F and its precession about B . B_{RF} is the RF magnetic field.

Consider the system as seen in a coordinate system that is rotating with about \mathbf{B} . The equation of motion is:

$$\frac{dF}{dt} = \gamma F \times B \quad (26)$$

The oscillating magnetic field can be considered to consist of two counter-rotating magnetic fields, and transformed to a coordinate system rotating about \mathbf{B} with angular frequency ω . Then:

$$\frac{dF}{dt} = \frac{\partial F}{\partial t} + \omega \times F \quad (27)$$

$$\frac{dF}{dt} = \gamma F \times B + F \times \omega = \gamma F \times \left(B + \frac{\omega}{\gamma} \right) \quad (28)$$

$$= \gamma F \times B_{eff} \quad (29)$$

where

$$B_{eff} = B + \frac{\omega}{\gamma} \quad (30)$$

In the rotating frame, the effect is the addition of a magnetic field ω/γ to the DC field \mathbf{B} . Consider the RF field to be composed of two counter-rotating components of which one has an angular velocity of $-\omega$ as shown in Figure 15. The effective magnetic field is given by:

$$|B_{eff}| = \left[\left(B - \frac{\omega}{\gamma} \right)^2 + H_{RF}^2 \right]^{1/2} = \frac{a}{\gamma} \quad (31)$$

where

$$a = \left[(\omega_0 - \omega)^2 + (\gamma B_{RF})^2 \right]^{1/2} = \left[(\omega_0 - \omega)^2 + \left(\frac{\omega_0 B_{RF}}{B} \right)^2 \right]^{1/2} \quad (32)$$

$$\omega_0 = \gamma B_0, \quad \cos \theta = \frac{\omega_0 - \omega}{a} \quad (33)$$

At resonance $\omega = \omega_0$, $\cos \theta = 0$ and $\theta = 90^\circ$.

$$\text{Also } a = \frac{\omega_0 B_{RF}}{B} \text{ and } |B_{eff}| = \frac{\omega_0 B_{RF}}{\gamma B} = \gamma B \frac{B_{RF}}{\gamma B} = B_{RF} \quad (34)$$

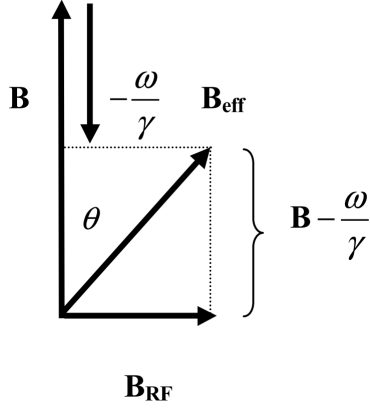


Fig. 15. Magnetic fields in the rotating coordinate system.

At resonance in the rotating frame, F precesses at the Larmor frequency about $\mathbf{B}_{RF} = \mathbf{B}_{eff}$. Off resonance, it precesses about \mathbf{B}_{eff} . This precession is equivalent to a change in the quantum number M or a transition between the M sublevels. At resonance, the Larmor frequency is $\nu = \gamma B_{RF}$, resulting in a period of $T = 1/\gamma B_{RF}$. At a given value of the RF magnetic field, the ratio of the periods of the two isotopes is $\frac{T_{87}}{T_{85}} = \frac{\gamma_{85}}{\gamma_{87}}$. In the present experiment we will only be interested in the situation at resonance.

Assume that the optical pumping has created an excess population in the $M = 2$ sublevel in the absence of RF. To the approximation used here, we will consider only the $M = 2$ and $M = 1$ sublevels, and neglect all effects of collisional relaxation. Assume now that the RF is applied at the resonance frequency. The situation is as depicted in Figure 16.

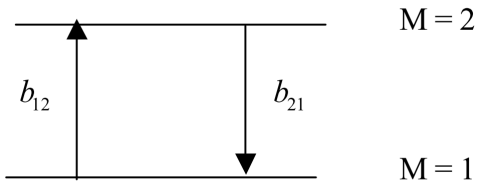


Fig. 16. RF transitions between the $M = 2$ and the $M = 1$ sublevels.

The arrows labeled b_{12} and b_{21} represent the transition probabilities from the $M = 1$ to the $M = 2$ and the $M = 2$ to the $M = 1$ sublevels respectively. The rate equations are:

$$\dot{p}_1 = -b_{12} p_1 + b_{21} p_2 \quad (35)$$

$$\dot{p}_2 = -b_{21} p_2 + b_{12} p_1$$

However, $b_{12} = b_{21} = b$. The equations are not independent. Therefore, we will consider only one of them, $\dot{p}_2 = -b p_2 + b p_1$, and the normalization condition $p_1 + p_2 = 1$.

Substitution yields:

$$\dot{p}_2 = b(1 - 2p_2) \quad (36)$$

The solution is:

$$p_1 = \frac{1}{2} - \delta e^{-2bt}, \quad p_2 = \frac{1}{2} + \delta e^{-2bt} \quad (37)$$

where δ represents the initial excess population in p_2 . At $t = 0$, $p_2 = 1/2 + \delta$ and approaches $1/2$ at $t = \infty$. Similarly, at $t = 0$, $p_1 = 1/2 - \delta$ and approaches $1/2$ at $t = \infty$. Thus the effect of the RF is to equalize the population of the two states. δ depends on the intensity of the optical pumping radiation and b is proportional to the current in the RF coils.

The above calculation suggests an exponential approach to the equal population condition. The situation is different, however, if the RF is suddenly turned on at the resonance frequency after the optically pumped equilibrium has been attained. Since the transition probability is the same for the up or down transition, and the initial population of the upper state is greater than that of the lower, the number of downward transitions will be greater than that of the upward and excess population will be created in the lower state. This will result in a rapid decrease in the intensity of the transmitted light.

Now the situation is reversed, and an excess population will again be transferred to the upper state resulting in a rapid increase in the intensity of the transmitted light. If the transmitted light intensity is being monitored as a function of time, a damped ringing signal will be observed, and the period of this ringing will correspond to the Larmor frequency for the precession of F about the RF magnetic field as seen in the rotating frame.

The above treatment neglects the effects of the other magnetic sublevels and also the effects of collisions between rubidium atoms and collisions between rubidium atoms and the buffer gas. However, the basic properties of the observed signal are described.

Before the RF is applied, the initial population of the p_2 state is $1/2 + \delta$. The time to reach $1/e$ of this value can be shown to be:

$$t_{1/e} = \frac{1}{2b} \quad (38)$$

Thus this time is inversely proportional to the RF perturbation and to the current flowing in the RF coils. It is instructive to measure this time as a function of the RF current.

II. EXPERIMENTAL SET-UP

(i) Rubidium Discharge Lamp

The rubidium discharge lamp consists of an RF oscillator, oven and gas bulb. The gas bulb is filled with a little rubidium metal and a buffer gas. The bulb sits within the coil of the oscillator (Figure 17). Stray ions within the bulb are accelerated by the RF electric fields caused by changing magnetic fields. Collisions between the accelerated ions and neutral atoms (both buffer gas atoms and vaporized *Rb* atoms) cause those atoms to be either ionized or to enter into an excited electronic state. Relaxation of the excited state by spontaneous emission results in the observed resonant radiation from the lamp. The bulb is heated in the oven to increase the *Rb* vapor pressure and also to regulate the lamp temperature. The oven temperature is set to $115^{\circ}\text{C} \pm 5^{\circ}\text{C}$.

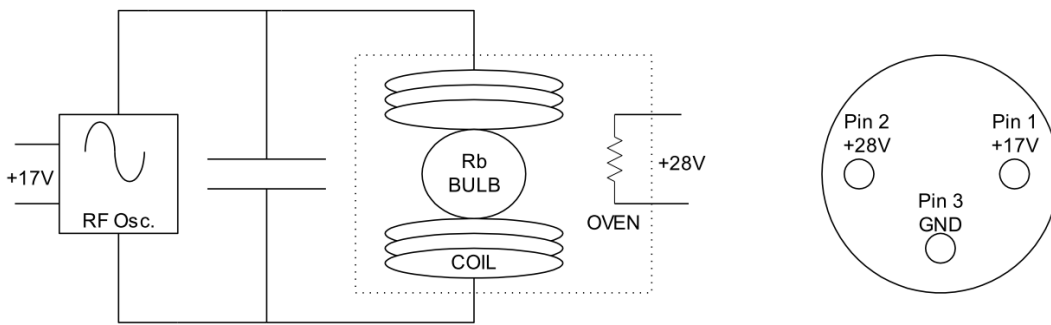


Fig. 17. Discharge lamp and back panel lamp connections.

The rubidium discharge lamp has been isotopically enriched with Rb^{87} . It is filled with 50% Rb^{87} and 50% natural *Rb*. Since rubidium in its naturally occurring isotopic concentration has 28% Rb^{87} and 72% Rb^{85} , the mixture in the lamp equates to about 36% Rb^{85} and 64% Rb^{87} . The buffer gas is xenon. This lamp is an optically extended source of light with radiation from both isotopes of rubidium and multiple lines from the buffer gas xenon.

Voltage is supplied to the lamp when the main power is turned on. Within a few minutes of applying power to the lamp, you should see the pinkish discharge light. The oven within the lamp takes 10 to 20 minutes to stabilize. It should be noted that the 795 nm spectral line that is used in the experiment is in the near infrared and cannot be seen by the human eye. The light that you see comes from other lines of rubidium and xenon.

(ii) Detector

The detector is a PDB-C108 silicon photodiode from Photonic Detectors Inc. The active area of the diode is circular, with a diameter of 1/4 inch. The spectral response at 795 nm is about 0.6 A/W. The diode is connected to a current to voltage preamplifier (see Figure 18). To determine the current supplied by the photodiode, divide the output voltage by the gain resistance. The diode is used in photovoltaic mode (cathode grounded, rather than reverse biased) for minimum noise. The preamp is a current-to-voltage converter with three gain settings selectable by the small switch on the front of the detector. It has a two-pole low-pass filter to roll off the high frequency gain at about 10 kHz. (see Table 1). The photodiode preamplifier has a voltage output of 0.0 to -11.5 V. It is important that the pre-amp

be operated at a gain setting such that the output is between -2.0 to -8.0 V to avoid saturating the pre-amp. Power connections to the preamp are by the black plastic connector to the front panel of the electronics box.

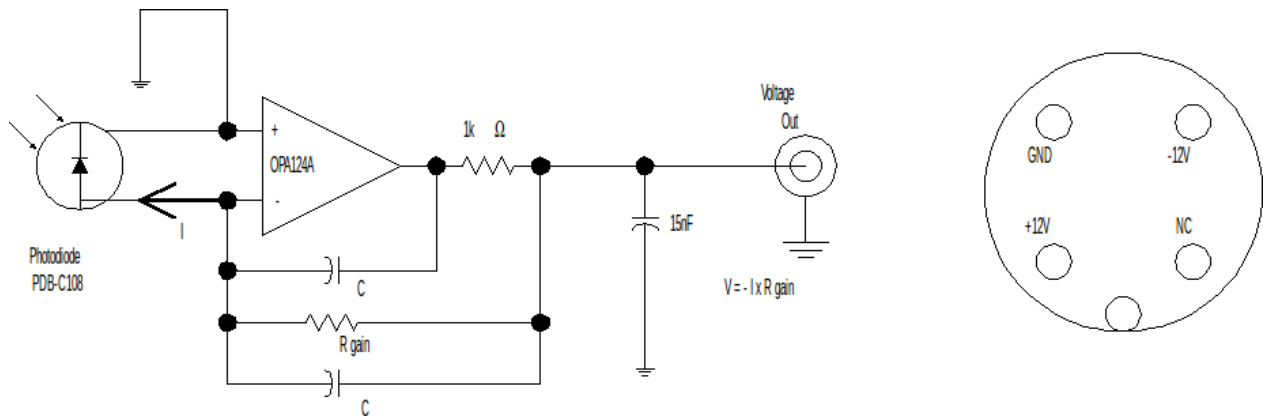


Fig. 18. Schematics of the photodiode preamplifier and preamp power connections.

Gain Resistor (MΩ) ± 5%	Low pass 3dB point (kHz) ± 10%	Noise (μV _{p-p})
1	12.0	20
3	8.0	40
10	5.0	100

Table 1. Photodiode preamplifier specifications.

The signal from the preamp is on the coaxial cable with BNC connector labeled Detector. This separate detector connector allows the student to observe the signal from the preamp directly on an oscilloscope. The signal from the preamp is negative with respect to ground.

Normally the preamplifier output will be plugged into the input of the detector section of the electronics box. The detector inverts the signal from the preamp so that more light appears as a larger voltage on the meter or detector output. The detector electronics consist of the following sections:

1. DC offset: 0-10 V DC Set by ten turn potentiometer and fine control approximately 0-20 mV set by a one turn potentiometer. The fine control will only be useful at the highest gain settings.
2. Gain: 1, 2, 5 ...100 Adjustable gain set by selector switch and ×1, ×10 set by toggle switch. Maximum gain is 1000.
3. Low Pass Filter: A two pole low pass filter with the following time constants; min., 1 ms, 10 ms, 100 ms, 1 s, 3 s. When set to min., the frequency response is determined by the gain setting of the preamplifier.
4. Meter: The meter displays the output voltage of the detector electronics. The range is -4 to +4 Volts with the meter multiplier toggle set to ×1, and -8 to +8 Volts when set to ×2.

There is 80 μV_{p-p} (referred to the input) of 60 cycle pickup noise on the detector output.

(iii) Optics

1. Two plano-convex lenses: Diameter 50 mm, focal length 50 mm. Plano-convex lenses minimize spherical aberrations when there are large differences in the object and image distance from the lens. For best use, the curved side should face towards the larger distance.

2. Interference filter: Diameter 50mm. The transmission characteristics of the filter are shown in Figure 19. We are mostly interested in the rubidium D lines at 780 nm and 795 nm that represent transitions between the ground state and the first excited state of rubidium. The transmission peak of the interference filter may be “tuned” to shorter wavelengths by rotation about the vertical axis. If λ_0 is the peak wavelength, then when the filter is tilted at an angle θ the new peak wavelength will be given by:

$$\lambda_s = \lambda_0 (1 - \sin^2 \theta / n^2)^{1/2} \quad (39)$$

where n is the index of refraction of the filter.

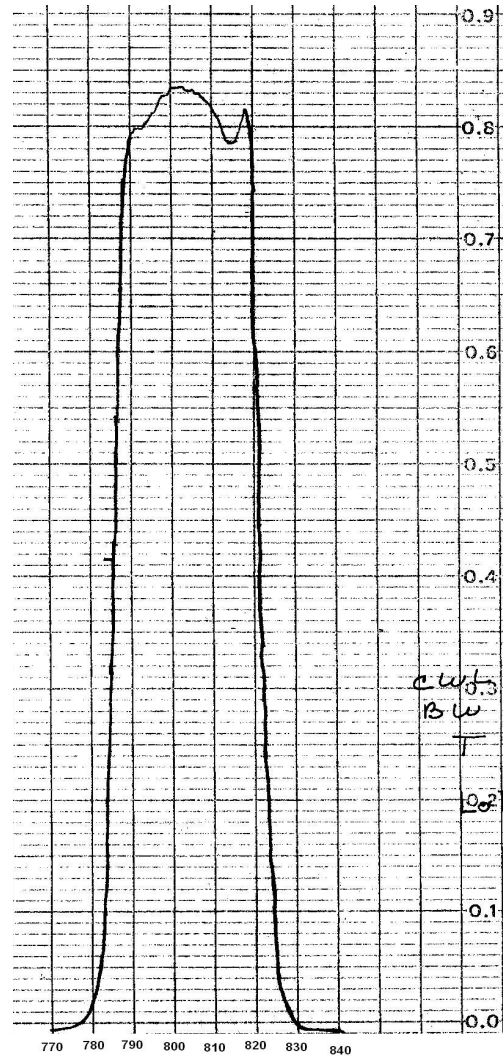


Fig. 19. Transmission of interference filter.

3. Two linear polarizers in rotatable mounts: Diameter 50 mm. Figure 20 shows the transmission and extinction characteristics of the polarizers. The linear polarizer mount has an alignment mark indicating the axis of polarization. The mark should be accurate to $\pm 5^\circ$.

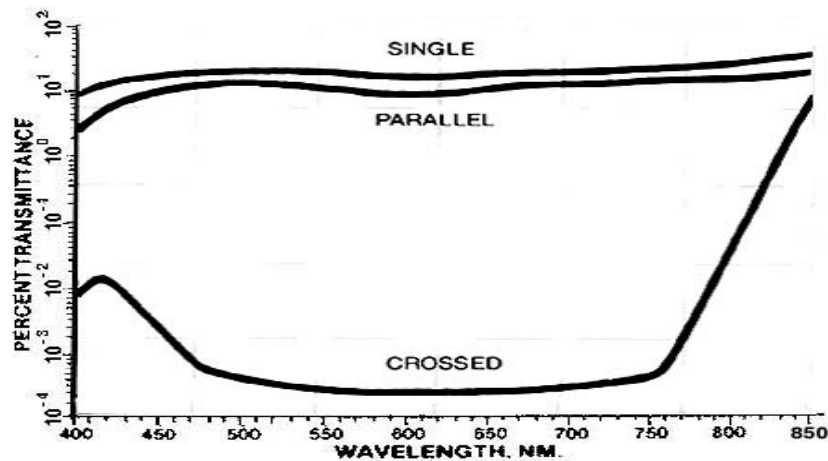


Fig. 20. Transmission characteristics of linear polarizers.

4. Quarter wavelength plate in rotatable mount: Diameter 50 mm, “optical thickness” 205 ± 5 nm. When properly oriented, the quarter wave plate allows linearly polarized light to be converted to circularly polarized light. The plate has two optical axes (at 90 degrees to each other) with different indices of refraction along each axis. Light travels at different speeds along each axis. The axes are called the “fast axis” and “slow axis”. To produce circularly polarized light, monochromatic linear polarized light is placed incident to the plate at 45° to each axis.

If the plate is of the correct thickness, then the phase lag along the slow axis causes the light exiting the plate to be circular polarized. The “optical thickness” of the plate may not be $795\text{nm}/4$, which is the desired value. Tuning the optical thickness (retardation) can be accomplished by rotating the plate about the vertical axis. Rotation about the slow axis increases the retardation, and about the fast axis decreases it. See Figure 21. This tuning method requires the fast or slow axis to be aligned vertically.

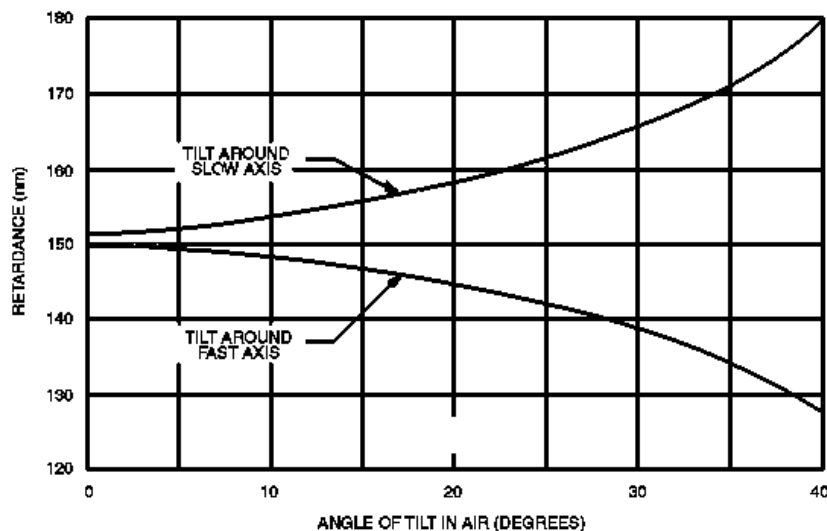


Fig. 21. Tilt tuning of quarter wave plate.

5. Alignment: During most of the alignment process, it is helpful to have the room lights dimmed to reduce stray light interference. You do need a little light to be able to see the components and detector meter. Note that the magnet coils are NOT centered on the optical rail. The short side is for the detector and the longer side is for the lamp and other optics. A ruler along one side of the optical rail will help with spacing the components.

The height of the experimental cell has been set so that its center is 3.5" above the optical rail. This means that you will want to set all the rest of the optics so their centers are also at this height. The optics elements can be rotated both about the z-axis (the direction along the optical rail) and the vertical axis (towards the center of the Earth) in the alignment process.

The lamp is located near the end of the long side of the optical rail, with its opening 3.5" above the rail. The lamp turns on as you switch the controller box on. It will take some time for the lamp to warm up.

Set the cell temperature to 20° C. (The exact temperature is not critical. However, we don't want the cell temperature to be set at some high temperature where there is very little transmission. Temperatures around 20° C work well for this part of the experiment.)

Place the photodiode detector at the far end of the optic rail on the opposite side of the cell from the light source. Set the center of the detector opening at 3.5" above the rail.

Set the gain on the photodiode detector to 1 M Ω (toggle switch down) and connect the photodiode detector to the electronics box. Set the electronics DC offset to zero and the gain to one.

Locate one of the plano-convex lenses so that its flat side is three to four centimeters from the front of the lamp. Because the lens has a focal length of 5 cm, this puts the center of the bulb at the focus of the lens. As a result, the emerging light will be collimated. We start here because the interference filter and 1/4 wave plate work best with approximately parallel light rays. A perfectly parallel beam cannot be created because the bulb inside the lamp is approximately 10 mm \times 15 mm. (If you want to see how well the lens actually works, you can try the following. Remove everything from the rail except the lamp and lens. Then, in a darkened room, observe how the shape and size of the beam spot change as you vary the lamp to lens separation.) Now adjust the height of the lens and its position along the rail to maximize the signal coming from the detector.

Place the second lens on the short side of the optical rail with its flat side towards the photodiode detector. The separation between the lens and detector carriers should be about 1-2 cm. Start with the lens centered at 3.5" above the rail and then adjust the position of this lens to maximize the signal from the photodiode detector. If you have done things correctly, you will find that there is so much light that the photodiode detector goes off scale. (The signal will be greater than 10 Volts.)

Put the rest of the optics into the beam path on the long side of the optical rail. The order should be lamp, lens, interference filter, linear polarizer, 1/4 wave plate, rubidium cell. This should attenuate the light enough so that you are not off scale. Again maximize the signal by adjusting the lenses.

6. Alignment of polarizers: The alignment marks on the linear and circular polarizers are accurate to $\pm 5^\circ$. The $1/4$ wavelength retarder may not be of exactly the right thickness. Careful alignment of these components can improve your signals by as much as 30%. However, this is not necessary to get a signal. For a quick alignment, set the linear polarizer at 45° and the $1/4$ wave plate at 0° or 90° . The light will need to go through the linear polarizer before it passes through the $1/4$ wave plate.

For a better alignment, remove the $1/4$ wave plate and set the first linear polarizer at 45° . Set the second linear polarizer in front of the detector and rotate it about the z-axis till you see maximum extinction, minimum signal. Typical “extinction” is about 2% of the maximum signal. The alignment mark on the second polarizer should be close to 135° or 315° (90° difference from first polarizer). Now place the $1/4$ wave plate after the first polarizer and rotate the wave plate about the z-axis till you see a maximum signal. The alignment mark should be near 0° , 90° , 180° , or 270° . You may now rotate the second linear polarizer about the z-axis, (using it as an analyzer) to determine the degree of circular polarization.

For complete circular polarization, there should be no change in the signal level as you rotate the second linear polarizer. Typical changes from maximum to minimum are between 0% to 50%. If there is a change in light level reaching the detector as you rotate the second linear polarizer, then you can “tune” the $1/4$ wave plate by rotation about the fast or slow axis. Rotate the $1/4$ wave plate slightly (5° – 10°) about the vertical axis. Now rotate the second linear polarizer again and observe the relative changes in the signal. If the relative change is worse than before, then the $1/4$ wave plate needs to be rotated 90° about the z-axis. Otherwise continue tilting the $1/4$ wave plate about the vertical axis and analyzing the result with the second linear polarizer.

For the absolute best in alignment (given the components available), one needs to correct for the slight differences between the alignment marks and the real position of the axes. There are several ways to do this. The way we choose to do this is by adjusting the first linear polarizer to 45° . We do this by observing that at exactly 45° , a rotation of 180° about the vertical axis is equivalent to a rotation of 90° about the z-axis.

Remove the $1/4$ wave plate and have in place only the two linear polarizers. Set the first linear polarizer for 45° . Rotate the second linear polarizer about the z-axis until you observe the minimum signal. Record the position of the second linear polarizer. Now flip the first linear polarizer (rotate 180° about vertical axis). Again rotate the second linear polarizer about the z-axis until you observe the minimum signal. Record the position of the second linear polarizer. If the difference in position from the first reading is 90° , then the first linear polarizer is at 45° to the vertical. If the difference is less than 90° , then increase the setting of the first linear polarizer by a few degrees (the amount you need to change it is exactly $1/2$ the difference between your readings of the second linear polarizer and 90°). If the difference is greater than 90° , then you need to decrease the angle of the first linear polarizer. After the first linear polarizer is set to 45° , follow the previous steps for alignment of the $1/4$ wave plate.

(iv) Temperature regulation

The following components make up the cell temperature regulation system:

1. Temperature regulator: Proportional, Integral, Derivate (PID) temperature controller with associated electronics.

2. Temperature probe: Type T (Copper - Constantan) Thermocouple (5 μm wire) {Constantan is magnetic and the small wire size was chosen such that the magnetic effects of the probe were unobservable, but the small wire size also makes the probe very delicate.}

3. Oven: The oven contains the following:

Rubidium cell: The cell is a glass cylinder with an outside length of 36 mm, outside diameter of 25 mm, and a wall thickness of about 1.5 mm. The cell contains rubidium metal with associated vapor and neon buffer gas at about 0.04 atm pressure.

Cell holder: A foam insert holds the cell in the center of the oven.

Heater: The heater is an open ended glass cylinder wrapped with non-magnetic bifilar wound heater wire. The resistance of the heater is about 50 Ω .

Insulation: A layer of foam insulation surrounds the heater.

Oven casing: The oven casing is a Plexiglas cylinder. The removable end caps contain 50 mm optical windows. Holes in the casing allow for the heater wire and thermocouple wire to enter the inside of the oven. An RF wiring box (discussed in the RF section) is attached to the oven casing.

4. Operation: The thermocouple plugs into the lower front panel and the heater is connected to the banana plugs next to it. The control system for the Omega temperature controller is mounted on the upper left of the front panel. Reading from left to right across the face of the unit, the three keys used to program the controller are MENU, UP and DOWN. Temperature is displayed in degrees Celsius.

Pressing the MENU key once displays “PRoC”, and after a brief delay, shows the current temperature. In this mode, you will be able to watch the measured temperature as it changes. Pressing the MENU key again displays “SP”, and after a brief delay, shows the temperature set point. Once the temperature set point is displayed, you can change it as desired using the UP and DOWN buttons.

The minimum temperature is set by the ambient room temperature. The maximum temperature of about 100° C is power limited by the 28 V power supply and the 50 Ω heater resistance. There is no need to worry about burning out the heater. There is simply not enough power to raise the temperature significantly above 100° C.

(v) Magnetic fields

All DC magnetic fields are produced by Helmholtz coil pairs. The coils are copper wire wrapped on phenolic bobbins. The following table lists their properties:

	Mean Radius (cm)	Turns/Side	Field/Amp ($T \times 10^{-4}/\text{Amp}$)	Maximum Field ($T \times 10^{-4}$)
Vertical magnetic field	11.735	20	1.5	1.5
Horizontal magnetic field	15.79	154	8.8	22.0
Horizontal magnetic field sweep	16.39	11	0.60	0.60

Table 2. Magnetic field values. The calibration of Field/Amp is only approximate.

A simplified schematic of the current regulated field control circuitry is shown in Figure 22. The circuit is a simple voltage-to-current converter. The reference voltage determines the voltage across the sense resistor and hence the current through the coils. The compensating network “tunes” out the coil inductance so that it appears as a pure resistance to the rest of the circuit. The compensating network draws no DC current.

The voltage across the sense resistor may be measured via tip jacks. The $100\ \Omega$ is in series so that the sense resistor cannot be accidentally shorted by the student. Connections to the coils are made by the front panel banana plugs. All the field controls are unipolar. If you wish to reverse the field direction, you must switch the front panel banana jacks.

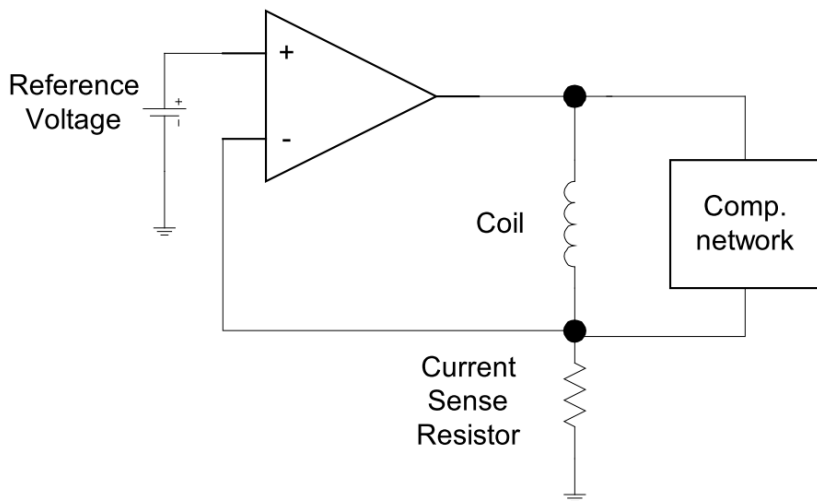


Fig. 22. Schematic of field control circuitry.

1. Vertical magnetic field: The vertical magnetic field is run between ground and the negative supply voltage. This is done because of the current limit of the power supply. The sense resistor is thus at -15 V with respect to ground. Caution should thus be exercised if this voltage is monitored with anything but a floating voltmeter.

Sense resistor: 1 Ω , 1%. Monitoring of the sense resistor is done through the back panel tip jacks.

Polarity: The vertical coil is wired so that field will point downward when the red jack is in the red plug. This is the correct direction to cancel the Earth's magnetic field in the Northern hemisphere. If you are in the Southern hemisphere, you should reverse the jacks. A current of about 0.33 Amperes will cancel the vertical field in Buffalo, NY. USA.

Control: The ten turn potentiometer sets the reference voltage. The maximum voltage is 1.0 Volt. (one turn = 0.1 Volt = 0.1 Ampere)

2. Horizontal magnetic field: The horizontal magnetic field can be run off the internal power supply with a maximum current of about 1.0 Ampere. An external power supply can be used to go to higher fields. The external power supply is connected to banana plugs on the back panel. A toggle switch on the back panel determines which supply is in use.

Sense resistor: 0.5 Ω , 1%. Monitoring of the sense resistor is done via front panel tip jacks.

Polarity: The horizontal magnetic field is wired such that the field will point from the lamp towards the detector (in the direction of light propagation) when the red plug is in the red jack.

Control: The ten turn potentiometer sets the reference voltage. The maximum voltage is 1.5 Volt. (one turn = 0.15 Volt = 0.3 Ampere)

External power: The following conditions must be obeyed when using an external DC power supply. The maximum voltage is 40 V. The maximum current is 3.0 A. (The circuitry is fuse protected.) The red banana plug must be connected to the positive terminal of the power supply. (The circuitry is diode protected against reverse polarity.)

There are a few other facts that the user should be aware of when using an external power supply. At room temperature, the main coil resistance is about 10 Ω . When large currents are used, coil temperature will increase (to about 75 °C at 2.7 A). This increase causes an increase in the resistance of the coils (to about 12 Ω at 75 °C). The changing coil resistance may cause the control circuitry to fall out of compliance. The large amount of heat being dissipated by the coils changes the thermal environment for the nearby cell and lamp. You may notice that it takes a long time for the cell temperature to stabilize. The temperature increase of the coil will also cause a change in the size of the copper coil. It might be instructive for the students to estimate the magnitude and sign of this change to determine if it would have any effect on their field calibration.

Error light: The error light will come on when the current regulated supply is close to being out of compliance (not enough voltage to supply the desired current). For efficient operation, when using an external power supply the voltage of the external power supply should be set a few volts above the point where the error light comes on. The pass element of the control circuitry (which is the power transistor mounted on the back panel heatsink) must dissipate all the excess power. In the worst case scenario the pass transistor will warm up to 90 °C. This is within transistor's specifications, but it will be happier and live a longer life if it is kept cooler.

3. Horizontal magnetic field sweep: We often refer to this field as just the sweep field. The sweep field coil is a single layer of wire wrapped on top of the horizontal magnetic field coils.

Sense Resistor: 1.0 Ω , 1%. Monitoring of the sense resistor is done via front panel tip jacks.

Polarity: The sweep field is wired such that the field will point from the lamp towards the detector (in the direction of light propagation) when the red plug is in the red jack.

Control: The reference voltage for the sweep field is the sum of three voltages; a start field voltage, a sweep voltage, and a modulation voltage. We will discuss each in turn. The maximum current that the sweep control can supply is about 1.0 A. When turned to full scale both the start field and sweep (range) voltage are about 1.0 V. This means that it is very easy to set the sweep control so that it is out of compliance. There is no error light to warn the students when this happens. They need to be alert to the possibility.

Start field: The ten turn potentiometer sets the start field voltage. The maximum voltage is about 1.0 Volt. (one turn = 0.1 Volt = 0.1 Ampere)

Sweep field: The sweep voltage is a voltage ramp that starts at zero volts and goes to the voltage set by the ten turn potentiometer marked "Range". The maximum range voltage is about 1.0 Volt. The ramp time is set by the selector switch marked "Sweep time". The sweep time may be set from 1 to 1000 seconds. Two toggle switches control when the ramp is started. When the "Start/Reset" toggle is at "Reset", the sweep voltage is zero. When the toggle is moved to "Start", the ramp is started. The "Single/Continuous" toggle determines what happens when the ramp finishes. When set to "Continuous", the sweep voltage will be reset to zero and then the ramp will repeat itself. If the "Single/Continuous" toggle is set to "Single", then at the end of the ramp the sweep voltage will remain at the voltage maximum voltage set by the range potentiometer. This is useful in setting up a sweep. With the toggle at "Reset" (or the range pot turned to zero), use the start field potentiometer to set the starting point for the sweep. Sweep quickly through the signal, and then use the range potentiometer to set the end of the sweep.

Ext. start: It is also possible to control the starting of sweeps electronically. The BNC labeled "Ext. start" on the lower front panel accepts TTL signals. With the "Start/Reset" toggle set to "Start", a positive TTL pulse (+5 V) on the "Ext. start" BNC will reset the sweep voltage to zero. On the falling edge of this pulse, the sweep voltage will start to ramp. If the controller is set to "Continuous", the ramp will reset at the end of the ramp and start again. If set to "Single", the ramp will stop after one sweep, and remain at the maximum voltage until the next pulse is received.

Modulation voltage: As has been stated previously, the reference voltage for the sweep field is the sum of three different voltages; the start field voltage, the sweep voltage, and the modulation voltage. The modulation voltage is derived from the controls labeled "Magnetic field modulation" on the upper front panel.

The controls consist of a BNC input, a "Start field /MOD" toggle switch, and a one turn potentiometer labeled "Amplitude". The modulation voltage has several uses. With the toggle switch set to "Start field", the BNC input is excluded from the circuit and a small DC voltage is supplied to one side of the

potentiometer. The modulation voltage (which is the voltage on the potentiometer wiper) is then some fraction of this DC voltage. The modulation voltage thus acts as a fine control of the start field. This is useful when you want to sit right on one of the dips in the rubidium spectrum.

With the “Start field/MOD” toggle in the “MOD” position, the voltage present on the BNC input is supplied to the potentiometer and becomes the basis for the modulation voltage with the following specifications:

Input impedance: 1 k Ω
Maximum voltage: ± 20 V
Voltage - Field conversion: 1 V \approx 100 μ T

The modulation input can be used for at least two different types of investigations. When used in conjunction with either Lock-in or AC detection methods, it allows students to do magnetic field modulation experiments. If large square wave signals are applied, the input can be used for field reversal experiments.

Recorder output and recorder offset: The recorder output is a signal derived from the 1 Ω sense resistor that is suitable for driving a chart recorder or oscilloscope. The voltage across the 1 Ω sense resistor has been amplified and passed through a low pass filter (time constant = 2 ms). The signal can also be given a DC offset with a ten turn recorder offset potentiometer which adds a negative DC voltage to the signal (-15 V at full scale). The voltage on the recorder output can go from -13.5 V to +13.5 V. When setting up the largest possible sweeps of the instrument, the student needs to keep the output within this range.

(vi) Radio frequency

The RF section consists of the following: RF coils, 50 Ω current sense resistor and RF amplifier (see Figure 23). The RF coils are located on the outside of the cell heater.

Coils: 3 turns/side, 18 gauge copper wire
Diameter: 6.45 cm
Separation: 10.80 cm (Not in Helmholtz configuration)
Inductance: 1.66 μ H
Parallel capacitance: 24 pF

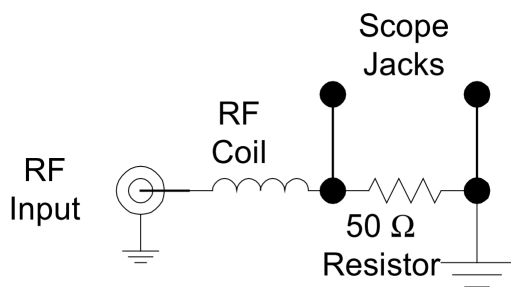


Fig. 23. RF coil and 50 Ω current sensing resistor.

The 50 Ω 0.5 Watt Current Sense Resistor is located in the electrical breakout box on the side of the cell. Oscilloscope probe jacks are on the side of the box so that you may measure the voltage across the resistor and thus measure the current in the coil. We have found that most scope probes are magnetic and would advise you to remove the probe after measuring the current. Because of the nuisance of attaching the probe to the sense resistor, the student may be tempted to simply measure the voltage at the output of the amplifier. Though this would be fine to measure relative changes in RF amplitude at one frequency, it will not give an accurate measurement of the current at high frequencies due to the effects of the long cable and finite coil impedance.

Radio frequency amplifier specifications:

Input impedance: 50 Ω

Output impedance: 15 Ω

Frequency range: 10 kHz - 30 MHz

Voltage gain: 6 V/V

Maximum output current: 100 mA

Maximum output voltage: 8 V_{p-p}

Maximum output power: 100 mW

Modulation input: TTL input, 0 V = RF on, 5 V = RF off

In addition to the input and output connections on the lower front panel, the RF amplifier has a single turn gain control to adjust the output amplitude and a TTL RF Modulation Input by which the RF can be modulated on and off. The modulation input can be used with a Lock-in amplifier or other AC detection technique. The output of the amplifier should be monitored with an oscilloscope to ensure that the amplifier is not being overdriven (clipped). A clipped RF output will lead to harmonics and spurious signals.

III. PROCEDURE

(i) Absorption of *Rb* resonance radiation by atomic *Rb*

In this first experiment, you will make an approximate measurement of the cross-section for the absorption of rubidium resonance radiation by atomic rubidium. The measured value will then be compared with the geometric cross-section and the value calculated from theory. The apparatus should be arranged as shown in Figure 24. The linear polarizer and the quarter wave plate should be removed since they will not be needed for this part of the experiment.

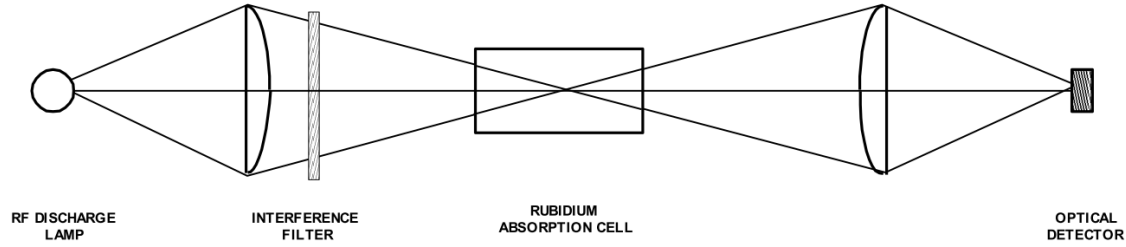


Fig. 24. Arrangement of the apparatus for studying the absorption of *Rb* resonance radiation by atomic *Rb*.

Check that the resistor selector on the optical detector at the end of the optical track is set to 1 M Ω . Set the detector amplifier gain on the front panel to 1, and its multiplier to $\times 1$. Check that the DC offset adjust knob is set to 0 V. Set the cell heater to 27 $^\circ$ C (300 K), and allow thermal equilibrium to be established. It will take about 30 minutes for the temperature to become stable. Connect the “Detector amplifier” output on the front panel to a DC voltmeter via a BNC cable and the appropriate adapter. Measure the intensity of the optical signal (in DC volts). Repeat the measurement in temperature increments of 10 $^\circ$ C up to 97 $^\circ$ C (370 K), taking care that thermal equilibrium is reached between readings.

Determine the density of atomic rubidium in the cell as a function of temperature from Table 3, and fit the data to an equation of the form:

$$I = I_0 e^{-\sigma \rho l} + C \quad (40)$$

where I_0 and I are the incident and outgoing flux of photons, ρ is the density of atomic rubidium in the cell, σ is the cross section, l is the path length through the rubidium cell (approximately 0.033 m), and C is an offset voltage due to various backgrounds. Determine the cross-section σ for the absorption of rubidium resonance radiation by atomic rubidium. Compare your result with the calculated value of the cross-section and with the geometrical cross-section.

Temperature (°C)	Temperature (K)	Density (Atoms/m ³)
17	290	3.3×10^{15}
27	300	1.1×10^{16}
37	310	2.9×10^{16}
47	320	7.5×10^{16}
57	330	1.8×10^{17}
67	340	4.3×10^{17}
77	350	8.3×10^{17}
87	360	1.5×10^{18}
97	370	3.7×10^{18}
107	380	6.3×10^{18}
117	390	1.2×10^{19}
127	400	2.4×10^{19}

Table 3. Density of rubidium atoms over solid or liquid rubidium as a function of temperature.

(ii) Low field resonances

In all of the following experiments in this lab manual, it will be necessary to apply a weak magnetic field along the optical axis of the apparatus. In order to do this satisfactorily, the apparatus must be located where the local residual magnetic field, which is due to the Earth's magnetic field and other magnetic objects in the vicinity of the experimental set-up, is as uniform as possible. Be sure to take this into account when you are in the lab. Moving lab stools or bumping the apparatus can alter results. Be especially careful with the lab stools; if possible, keep them on the opposite side of the room. All magnetic objects should be removed from the vicinity of the apparatus.

The optical axis of the apparatus should be oriented approximately along the horizontal component of the residual magnetic field in the lab (you will achieve fine alignment when working on the zero field transition). The apparatus should be set up as shown in Figure 25. **Be sure that the linear polarizer is placed before the quarter wave plate in order to obtain circularly polarized light, and that the two are oriented properly.**

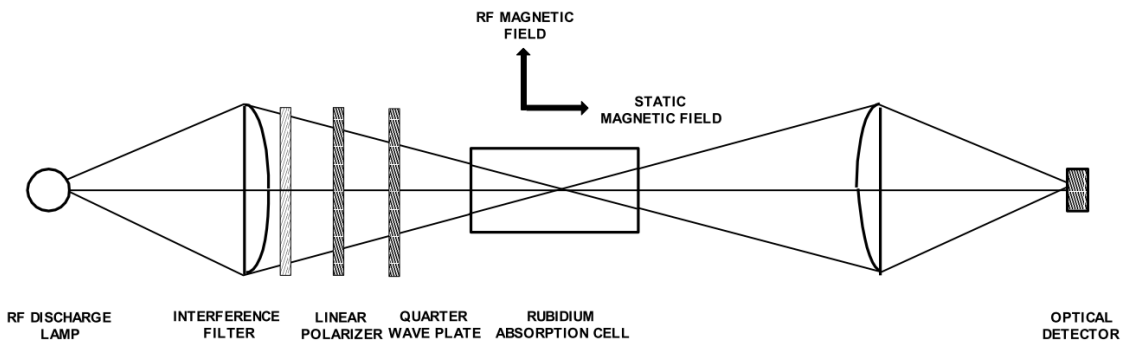


Fig. 25. Arrangement of the apparatus for optical pumping.

The magnetic fields will be determined approximately from the geometry of the field coils. All magnetic field coils in this experiment are in the Helmholtz configuration, and the magnetic field at the center of their common axis is given by:

$$B = \frac{8 \mu_0 N I}{\bar{R} \sqrt{125}} \quad (41)$$

where μ_0 is the permeability of free space ($4\pi \times 10^{-7}$ Henry/m), N is the number of turns on each side, I is the current in amps, and \bar{R} is the mean radius of the coils. The parameters N and \bar{R} for different coils in the apparatus can be seen in Table 2. For your report, produce plots of B as a function of I for each of the vertical magnetic field, horizontal magnetic field, and horizontal magnetic field sweep coils using their respective parameters from Table 2.

During the experiment, the currents I for horizontal magnetic field and horizontal magnetic field sweep coils can be measured using their monitor terminals on the front panel. At the “Horizontal magnetic field sweep” monitor, the current passes through a 1 Ω resistor and therefore a voltage is presented that is numerically equal to the current in amps. At the “Horizontal field” monitor, the current passes through a 0.5 Ω resistor and therefore a voltage is presented that is numerically twice the current in amps. The “Vertical field” monitor is in the back panel. It uses a 1 Ω sense resistor.

1. Zero field transition: Figure 26 shows the zero field transition. In order to observe the zero field transition, no RF is applied, and the current in the horizontal magnetic field sweep coils is slowly varied. Optical pumping is a slow process. Therefore, during these experiments, it will be necessary to use a slow sweep time setting (~ 10 s or more) for the horizontal magnetic field sweep. A useful trick is to set the sweep time to a lower setting (1-2 s) while searching for resonances, and back to higher settings (~ 10 s or more) when you are ready to take data.

Set the horizontal magnetic field current to zero using its control knob. Set the Time constant to 100 ms. Set the RF amplifier gain to 3 on dial. Check that the “Recorder offset” knob is all the way to the right, and leave it there for the duration of the experiment. Set the cell temperature to 50° C and allow thermal equilibrium to be established. It is most convenient if a signal proportional to horizontal magnetic field sweep coil current (“Recorder output” on the front panel) is displayed on the horizontal axis of the oscilloscope (CH1 in XY mode), and the output of the optical detector (“Detector amplifier” output on the front panel) is displayed on the vertical axis of the oscilloscope (CH2 in XY mode).

The “Start field” knob sets the starting value of the Horizontal magnetic field sweep, and the “Range” knob sets its maximum limit. Initially while looking for the zero field transition, set the “Start field” knob to 0, and the “Range” knob to its maximum value to cover the full available range. Once you find it, you can set the “Start field” and “Range” knobs as needed to observe the transition more clearly on the scope screen. Note that the horizontal magnetic field sweep in our set-up occasionally gets stuck. If you suspect that is happening, flip the horizontal magnetic field sweep selector switch to “Reset”, and then back to “Start”.

After observing the zero field transition, achieve minimum signal full-width-half-maximum (FWHM) by adjusting the current in the vertical magnetic field coils, and by moving the apparatus very slowly about its vertical axis to set it exactly along the horizontal component of the residual magnetic field in the lab. Aim to get a signal FWHM < 500 mV (Fig. 26). **Take a screenshot for your report. (Insert a USB Flash drive, and hit the “Save” button on the front panel of the oscilloscope. This will save the current screen on the drive as a .bmp image.)**

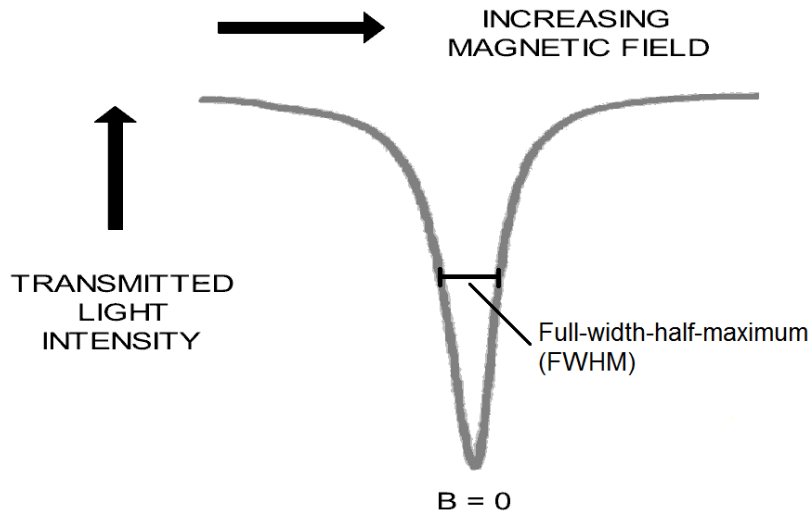


Fig. 26. Zero field transition. Scope is in XY mode (Display → Format → XY), CH1 500 mV/div and CH2 20 mV/div, detector amplifier gain is set to 1 with a $\times 1$ multiplier.

Now, you will measure the sweep field current that exactly cancels the residual magnetic field in the lab. Set the sweep field current mode from “Start” to “Reset”. As you observe the signal trace on the scope screen, trace the zero field transition manually with the “Start field” knob. Adjust the current to the center of the zero field transition, and measure the current using a DC voltmeter connected to the “Horizontal magnetic field sweep” monitor port on the front panel. From this and Equation 41, calculate the value of the horizontal component of the residual magnetic field in the lab. Measure the current on the vertical field coils using a DC voltmeter connected to the “Vertical field” monitor port in the back panel. From this and Equation 41, calculate the value of the vertical component of the residual magnetic field in the lab.

2. Measurement of g_F factors and nuclear spins: There are two isotopes of rubidium, Rb^{87} and Rb^{85} , and they have different nuclear spins. We are going to treat their values as unknowns and try to measure them. In order to do this, we must measure the g_F values from which the spins can be calculated. This can be done by measuring a single resonant frequency of each isotope at a known value of the magnetic field.

An RF signal is essentially a sine wave with frequency in the 3 kHz to 300 GHz range. Set the signal generator to produce an RF signal (a sine wave) at 100 kHz with 1.0 V amplitude. Connect this signal to the RF Amplifier Input port on the front panel to apply it on the RF coils in the apparatus. Set the RF amplifier gain to 3 using the knob on the upper left of the front panel.

Check that the horizontal magnetic field current is set to 0 at the “Horizontal magnetic field” adjust knob. Start the current in the sweep coils by flipping the selector switch from “Reset” to “Start”, and search for the Zeeman resonances (Figure 27). **Once you observe them, take a screenshot for your report.** Then, set the mode back to “Reset”. As you observe the signal trace on the scope screen, trace the Zeeman resonances manually using the “Start field” knob. Measure the horizontal magnetic field and horizontal magnetic field sweep currents at which each Zeeman resonance occurs with DC voltmeters at the respective monitor ports on the front panel. Repeat your measurements up to RF frequencies of 1 MHz in 50 kHz increments, increasing the current on the horizontal magnetic field coils as necessary.

Tabulate your results, indicating resonance frequencies for each Rb isotope, horizontal magnetic field current, horizontal magnetic field calculated from eq. 41, sweep field current, sweep field calculated from eq. 41, the horizontal component of the residual magnetic field in the lab (the vertical component is canceled by the vertical field coils), and the net magnetic field. Plot resonance frequencies as a function of net magnetic field for Rb^{87} and Rb^{85} on the same plot. Find the g_F factors of the two isotopes from the slopes of the lines using eq. 19. Find the corresponding nuclear spins using eq. 8. Compare your measurements with that predicted by theory.

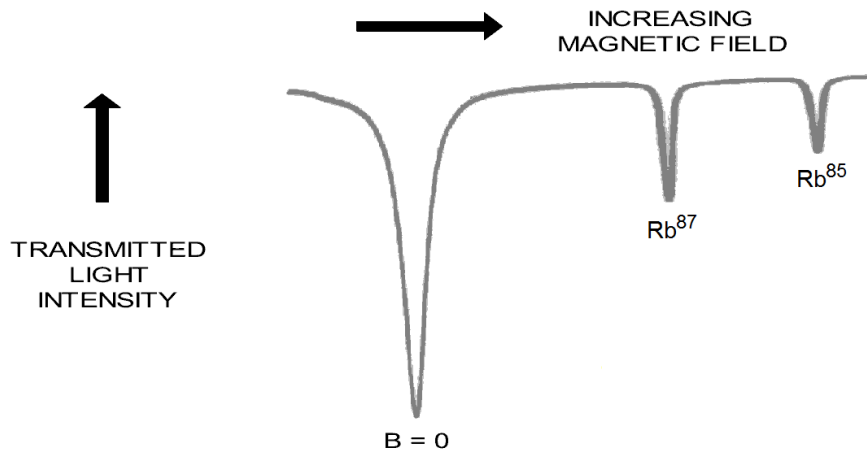


Fig. 27. Zero field transition and Zeeman resonances of Rb^{87} and Rb^{85} at low magnetic fields, RF is applied at a frequency of 100 kHz. Scope is in XY mode (Display \rightarrow Format \rightarrow XY), CH1 2 V/div and CH2 20 mV/div, detector amplifier gain is set to 1 with a $\times 1$ multiplier.

(iii) Quadratic Zeeman effect

The Zeeman resonances of both isotopes will now be studied as the applied magnetic field is increased into a region where the energy level splitting is no longer linear in B (see Fig. 7). Each of the zero field energy levels splits into $2F+1$ sublevels, whose spacing is no longer equal. In this region, there are $2F$ resonances whose splittings can be resolved. Thus, for $I = 3/2$ there are a total of six resonances with $\Delta F = 0$ and $\Delta M = \pm 1$, and for $I = 5/2$ a total of ten. Their relative intensities depend on the pumping conditions.

The magnetic field at which these resonances can be observed can be approximately determined from the resonance equation (eq. 19, $\nu = g_F \mu_B B/h$), and the current for the horizontal magnetic field coils set accordingly.

Use the values suggested below to look for Zeeman resonances at higher magnetic fields for Rb^{87} and Rb^{85} (Fig. 28 and 31). Use the Horizontal magnetic field sweep “Start field” and “Range” knobs as needed to observe the resonances clearly on the scope screen. Then, for each isotope, measure the sweep field current that corresponds to each resonance dip by manually tracing the signal. Calculate the net magnetic field at each location. Produce plots similar to Figure 29 and 32 from your data. If you can't see the resonances at suggested frequencies, vary the frequencies slowly around suggested values and try again. **Remember to take screenshots of the resonances for your report.**

Rb^{87} : Detector amplifier gain = 20, Multiplier = $\times 10$

$\nu \approx 6.0$ MHz

Time constant = 100 ms

RF amplifier gain = 3 on dial

Sweep time = 50 s

Horizontal magnetic field current = 1.0 amp (0.5 V on the monitor port, since $R=0.5 \Omega$)

Oscilloscope: XY mode (Display \rightarrow Format \rightarrow XY), CH1 500 mV/div and CH2 200 mV/div.

An example spectrum for Rb^{87} is shown in Figure 28, and the spectrum calculated from the Breit-Rabi equation is shown in Figure 29.

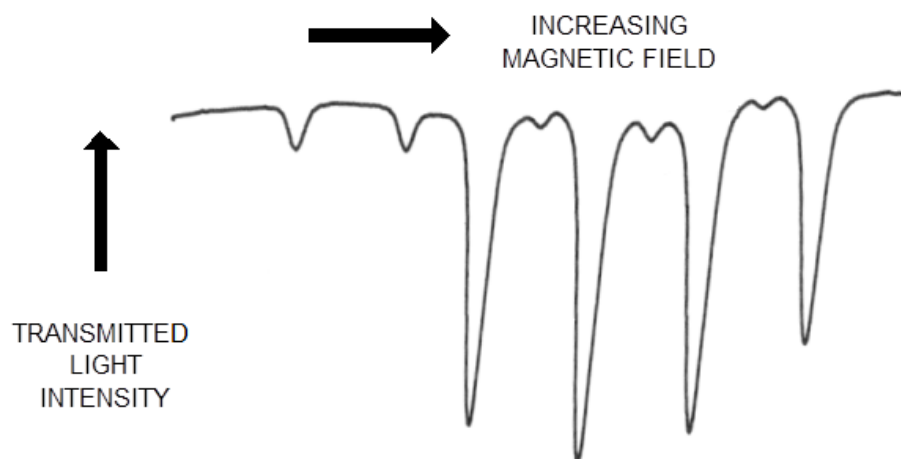


Fig. 28. Spectrum of Rb^{87} at optimum RF power. Note that the first two small dips in this example spectrum aren't visible in our set-up.

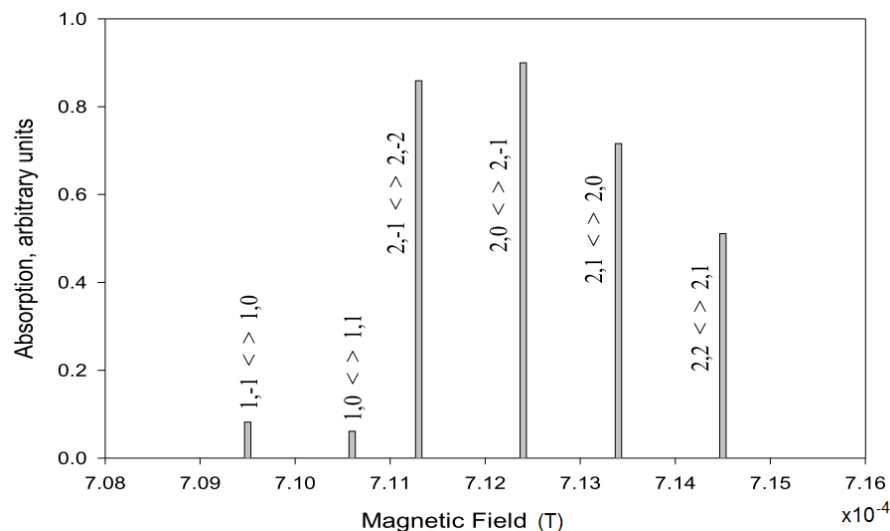


Fig. 29. Spectrum of Rb^{87} calculated from the Breit-Rabi equation.

Absorption intensities in Figure 29 have been adjusted to match the observed spectrum. The Breit-Rabi equation can not be directly solved for x and hence B , but it can be easily solved by a computer program. The results in Figure 29 were obtained using Maple.

Figure 30 shows the Rb^{87} spectrum taken under the same conditions as above, except at higher RF power (the signal generator is set to produce a 2.5 V amplitude sine wave this time). Here the double quantum transitions, which are radiative transitions between two states through the simultaneous emission or absorption of two or more photons, are visible midway between the single quantum transitions. Notice that the single quantum transitions have become broader because they are being overdriven by the higher RF power.

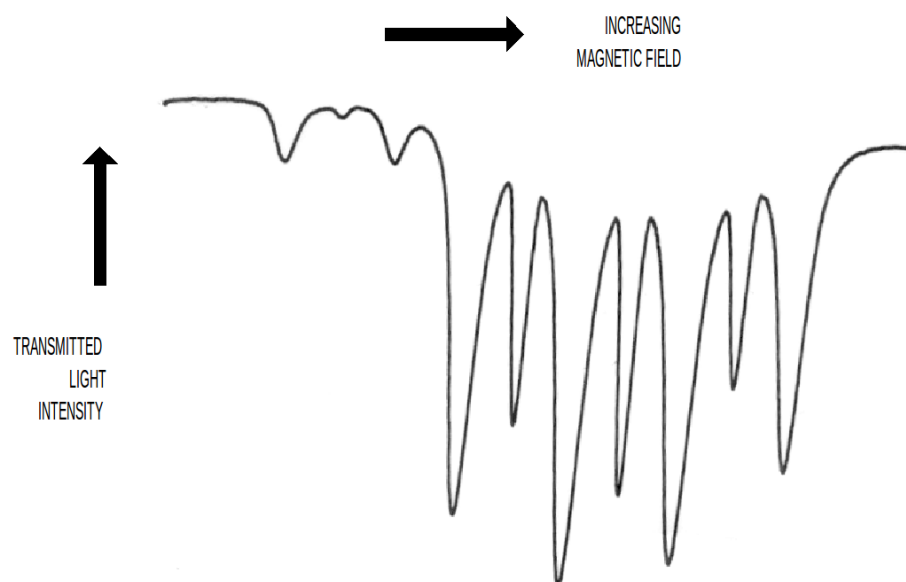


Fig. 30. Spectrum of Rb^{87} at higher RF power showing double quantum transitions. Note that the first two small dips in this example spectrum aren't visible in our set-up.

Rb^{85} : Detector amplifier gain = 20, Multiplier = $\times 10$
 $\nu \approx 4.1$ MHz
Time constant = 100 ms
RF amplifier gain = 3 on dial
Sweep time = 50 s
Horizontal magnetic field current = 1.0 amp (0.5 V on the monitor port, since $R=0.5 \Omega$)
Oscilloscope: XY mode (Display \rightarrow Format \rightarrow XY), CH1 1 V/div and CH2 200 mV/div.

An example spectrum for Rb^{85} is shown in Figure 31 and the spectrum calculated from the Breit-Rabi equation is shown in Figure 32.

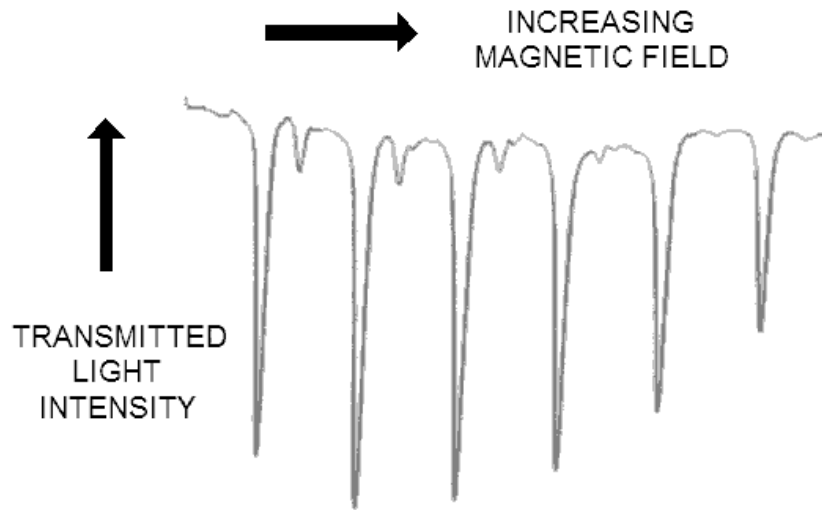


Fig. 31. Spectrum of Rb^{85} at optimum RF power.

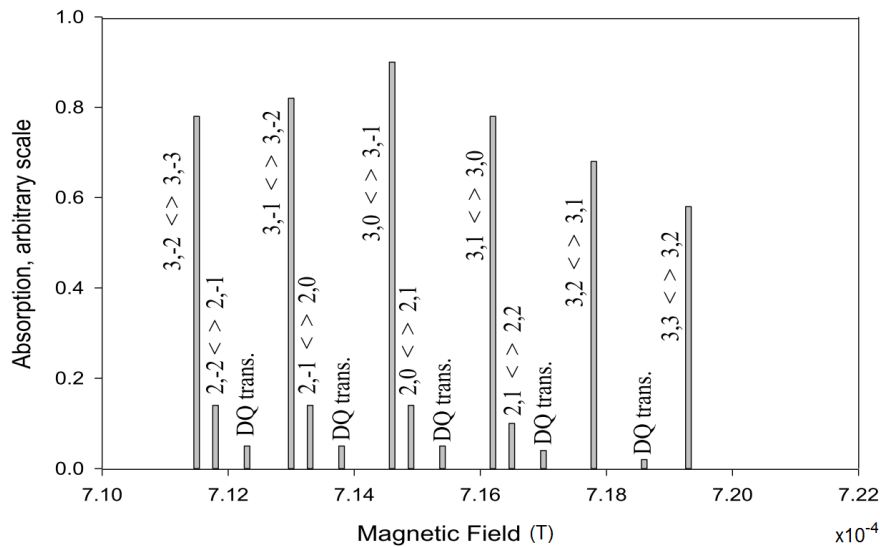


Fig. 32. Spectrum of Rb^{85} calculated from the Breit-Rabi equation.

Figure 33 shows the Rb^{85} spectrum taken under the same conditions as above, except at higher RF power (the signal generator is set to produce a 2.5 V amplitude sine wave this time). Once again, double quantum transitions are observed midway between the single quantum transitions.

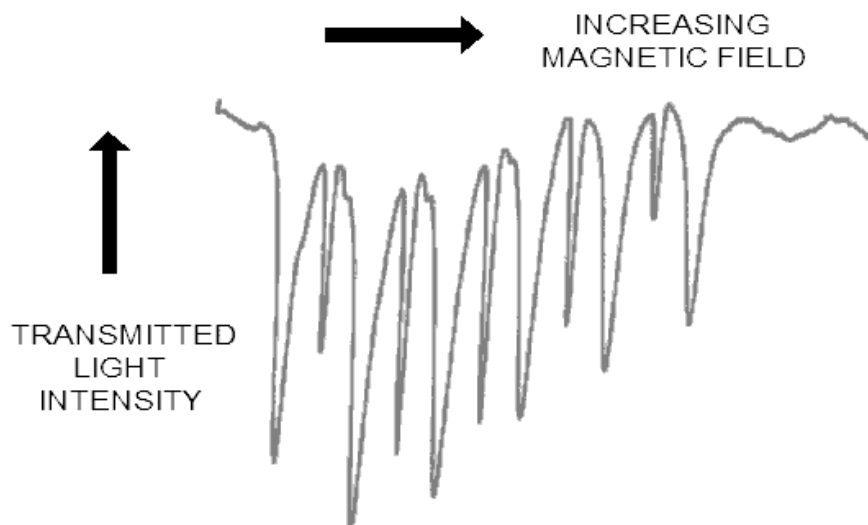


Fig. 33. Spectrum of Rb^{85} at higher RF power showing double quantum transitions.

(iv) Transient effects

In order to observe transient effects, it is necessary to either turn the pumping light on and off rapidly or turn the RF on and off while tuned to the center of a resonance. Here we will do the latter while tuned to the center of a low field resonance, and observe the transmitted light intensity as a function of time.

For this part of the experiment, be sure to turn the room lights off. Most room lights flicker at the 60 Hz AC mains frequency, and that may appear as unwanted oscillations in your measurements.

Start by finding Zeeman resonances for an arbitrary frequency, let's say 100 kHz. Set the "Detector amplifier" gain to 1 with a $\times 1$ multiplier. Set the "RF amplifier" gain on the front panel to 8. Set the "Time constant" on the front panel to min. Set the signal generator to produce a 100 kHz sine wave with 1.0 V amplitude. Connect this signal to the RF Amplifier Input port on the front panel. Once you observe the resonances, set the sweep field mode from "Start" to "Reset", and using the "Start field" adjust knob, set the sweep field to the middle of the Zeeman resonance for either Rb^{87} or Rb^{85} .

Now, set the second channel of the signal generator to produce a 5.0 Hz square wave with 5.0 V amplitude. Connect this wave to the "RF modulation" input on the front panel. Using a T connector, also connect the wave to CH1 on the scope. Connect the "Detector amplifier" output on the front panel to CH2 on the scope to monitor transmitted light intensity. **Take a screenshot of the two waves for your report.** Sample data is shown in Figure 34. The upper trace is the square waveform that is modulating the RF, and the lower trace is transmitted light intensity.

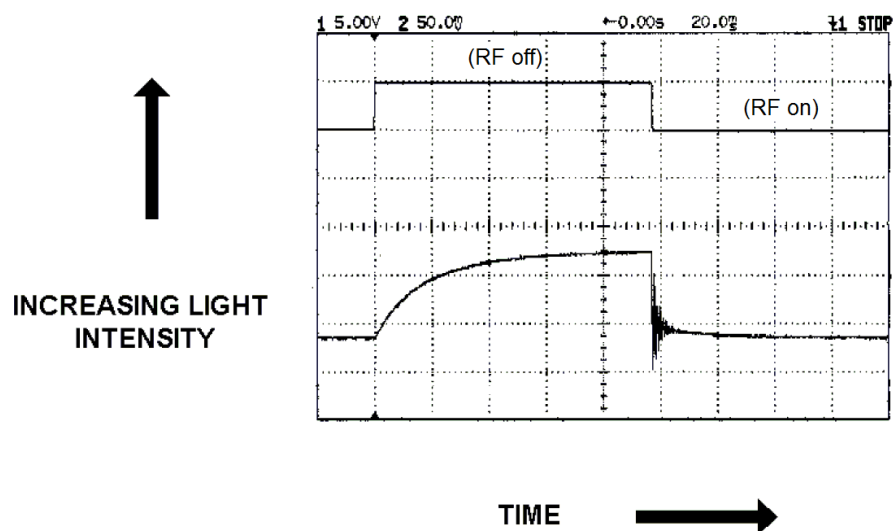


Fig. 34. Square wave modulating the RF (upper trace), and transmitted light intensity (lower trace).

RF is turned off when the square wave amplitude at the RF modulation input is > 0 V. Turning off the RF allows pumping to begin, and the light intensity increases exponentially until a maximum value is reached. The time constant of this exponential is a measure of the optical pumping time. The characteristic value of the time will be found to be proportional to the intensity of the pumping light. When the RF is turned on (the square wave amplitude at the RF modulation input is ≤ 0 V), RF causes transitions between the Zeeman sublevels, and the population of the levels are driven toward equilibrium. If the rise time of the RF envelope is short enough, the populations will overshoot, giving rise to the ringing shown in Figure 35 (this figure amplifies the region where the RF is turned on in Figure 34). The ringing damps out, and the light intensity drops to a minimum approaching that for the unpumped cell.

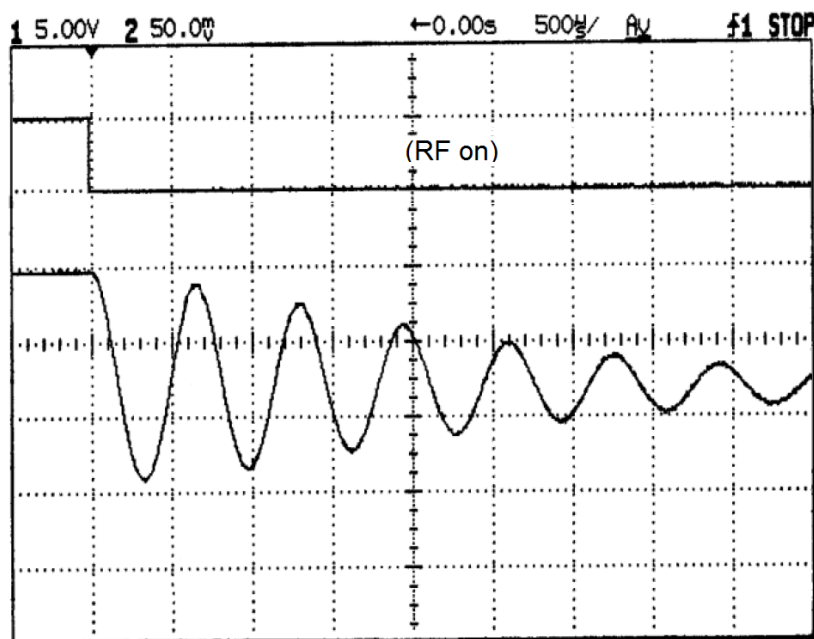


Fig. 35. The region where the RF is turned on in Figure 34.

The period of oscillations should be linearly proportional to the reciprocal of the amplitude of the RF, since it corresponds to the precession of \mathbf{F} about the RF magnetic field. Measure the change in the period of ringing as a function of RF signal amplitude for each isotope of Rb (you will need to set the sweep field to the middle of the Zeeman resonances for Rb^{87} and Rb^{85} , and follow the above procedure for each case). In order to do this, vary the sine wave amplitude on the signal generator in small steps such as 0.2 V, and measure the period of ringing for several different amplitudes. **Remember to take screenshots for your report.** Figure 36 shows some sample data. At a given value of the RF magnetic field, the ratio of the periods of the ringing goes inversely as the g_F factors, and the data shows that this ratio is $989/641 = 1.54$, whereas the theoretical value is 1.50.

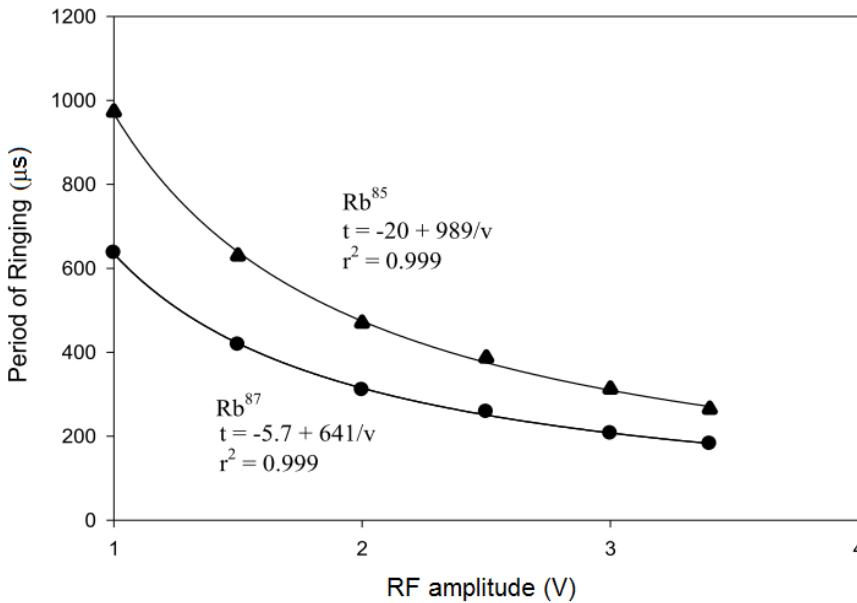


Fig. 36. Period of ringing vs. RF amplitude.

IV. FOR YOUR REPORT

(i) Your report should be in the general format of a scientific journal article, similar to the articles posted on UB Learns along with this lab manual. However, the individual sections should include a lot more detail, and the discussions should reflect how well you understand the theory and the experiment.

(ii) In the abstract, briefly summarize the procedures and your findings in the experiment. Highlight any important finding. Provide numerical results with errors where applicable.

(iii) In your own words, provide a detailed discussion of the theory behind the experiment.

(iv) Describe your experimental set-up, using clearly labeled figures where necessary. Your description should have sufficient detail to enable experimenters elsewhere to replicate your experiment.

(v) Present your data and discuss your results. Use tables and plots where necessary. For this experiment, remember to include:

- a plot of the density of atomic rubidium in the cell as a function of temperature, including an exponential fit to data.
- a plot of light intensity as a function of the density of atomic rubidium in the cell, including an exponential fit to data.
- plots of B as a function of I for the vertical magnetic field, horizontal magnetic field, and horizontal magnetic field sweep coils using the respective parameters from Table 2
- screen capture of the zero field transition
- screen capture of the zero field transition and Zeeman resonances of Rb^{87} and Rb^{85}
- a plot of Zeeman resonance frequencies vs. net magnetic field for Rb^{87} and Rb^{85}
- screen captures of spectra of Rb^{87} and Rb^{85} at optimum RF power showing the quadratic Zeeman effect
- plots of absorption versus net magnetic field for the quadratic Zeeman effect for Rb^{87} and Rb^{85}
- screen captures of spectra of Rb^{87} and Rb^{85} at higher RF power showing double quantum transitions
- screen capture showing the square wave modulating the RF and the transmitted light intensity
- screen capture showing the ringing pattern in the region where the RF is turned on
- a plot showing the change in the period of ringing as a function of RF amplitude for both Rb isotopes

Compare your experimental data with theoretical data where possible. Include sources of error and your error calculations in your discussions.

(vi) In your conclusions, summarize your findings. Discuss their relevance to theoretical expectations.

(vii) Cite all your references properly in the references section.